

183  
1/16/77

DR. 2428

# **Aerodynamic Resistance Reduction of Electric and Hybrid Vehicles**

## **A Progress Report—September 1978**

**Published April 1979**

**Under Contract No. NAS7-100, RD-152, Amendment No. 170**

Prepared for:  
**U.S. Department of Energy**  
Assistant Secretary for Conservation  
and Solar Applications  
Office of Transportation Programs

**MASTER**

Available from:

National Technical Information Service (NTIS)  
U.S. Department of Commerce  
5285 Port Royal Road  
Springfield, Virginia 22161

Price: Printed Copy: \$6.00  
Microfiche: \$3.00

## **DISCLAIMER**

**This report was prepared as an account of work sponsored by an agency of the United States Government. Neither the United States Government nor any agency thereof, nor any of their employees, makes any warranty, express or implied, or assumes any legal liability or responsibility for the accuracy, completeness, or usefulness of any information, apparatus, product, or process disclosed, or represents that its use would not infringe privately owned rights. Reference herein to any specific commercial product, process, or service by trade name, trademark, manufacturer, or otherwise does not necessarily constitute or imply its endorsement, recommendation, or favoring by the United States Government or any agency thereof. The views and opinions of authors expressed herein do not necessarily state or reflect those of the United States Government or any agency thereof.**

---

## **DISCLAIMER**

**Portions of this document may be illegible in electronic image products. Images are produced from the best available original document.**

# **Aerodynamic Resistance Reduction of Electric and Hybrid Vehicles**

## **A Progress Report—September 1978**

**Published April 1979**

**Prepared by:**  
**Jet Propulsion Laboratory**  
**Pasadena, California**  
**Under Contract No. NAS7-100, RD-152, Amendment No. 170**

**NOTICE**

This report was prepared as an account of work sponsored by the United States Government. Neither the United States nor the United States Department of Energy, nor any of their employees, nor any of their contractors, subcontractors, or their employees, makes any warranty, express or implied, or assumes any legal liability or responsibility for the accuracy, completeness or usefulness of any information, apparatus, product or process disclosed, or represents that its use would not infringe privately owned rights.

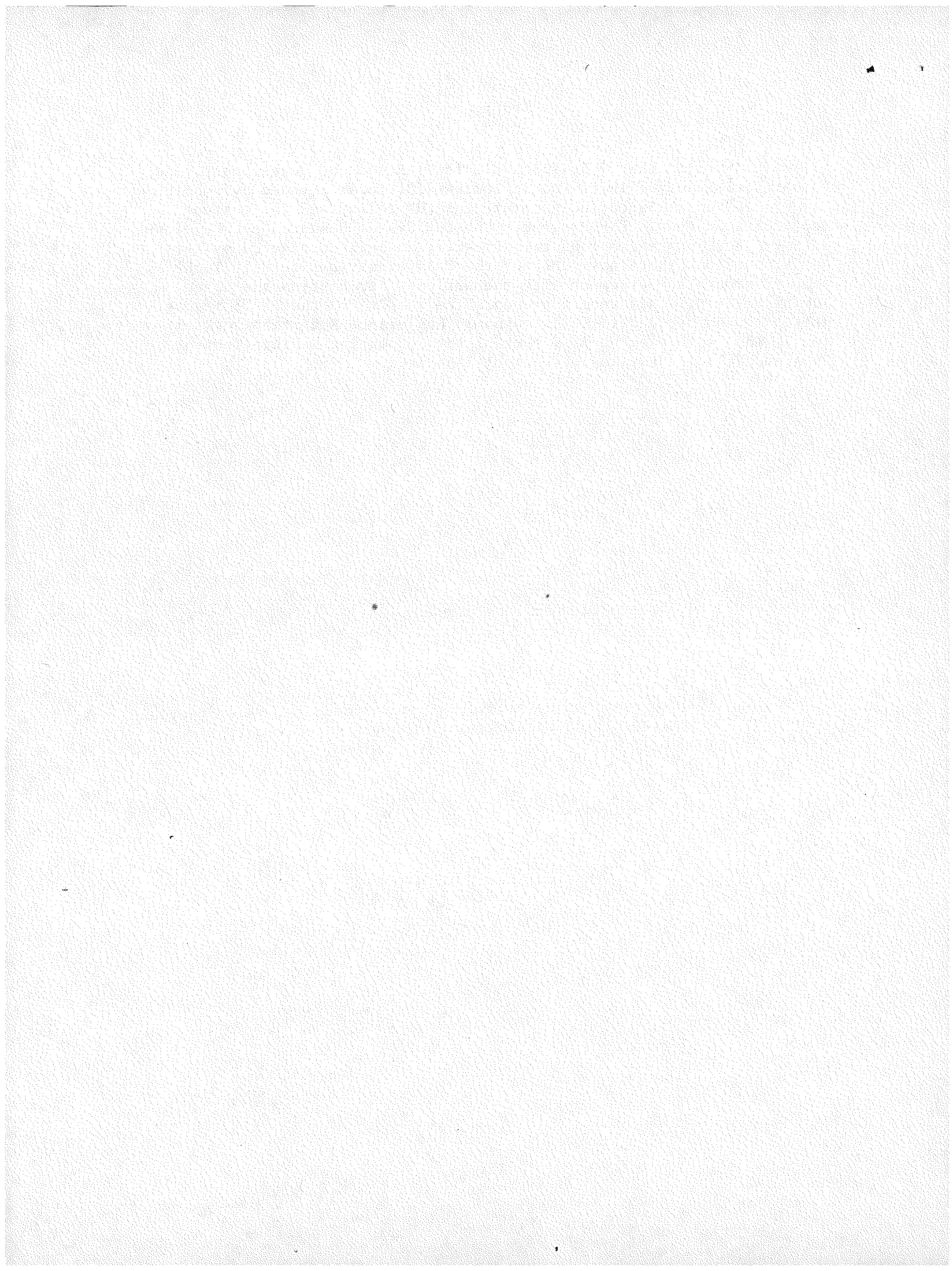
**Prepared for:**  
**U.S. Department of Energy**  
**Assistant Secretary for Conservation**  
**and Solar Applications**  
**Office of Transportation Programs**  
**Washington, D.C. 20545**

### NOTICE

This report was prepared as an account of work sponsored by the United States Government. Neither the United States nor the United States Department of Energy, nor any of their employees, makes any warranty, express or implied, or assumes any legal liability or responsibility for the accuracy, completeness, or usefulness of any information, apparatus, product, or process disclosed, or represents that its use would not infringe privately owned rights. Reference herein to any specific commercial product, process, or service by trade name, mark, manufacturer, or otherwise, does not necessarily constitute or imply its endorsement, recommendation, or favoring by the United States Government or any agency thereof. The views and opinions of authors expressed herein do not necessarily state or reflect those of the United States Government or any agency thereof.

## PREFACE

The Electric and Hybrid Vehicle (EHV) Research, Development, and Demonstration Act of 1976, Public Law 94-413, later amended by Public Law 95-238, established the governmental EHV policy and the current Department of Energy EHV Program. The EHV System Research and Development Project, one element of this Program, is being conducted by the Jet Propulsion Laboratory (JPL) of the California Institute of Technology through an agreement with the National Aeronautics and Space Administration. This report presents the results of the FY'78 investigations conducted under the Aerodynamic Resistance Reduction work element. This work element is a part of the Supporting Vehicle Technology Task and Vehicle Systems Development Task Area.



## SUMMARY

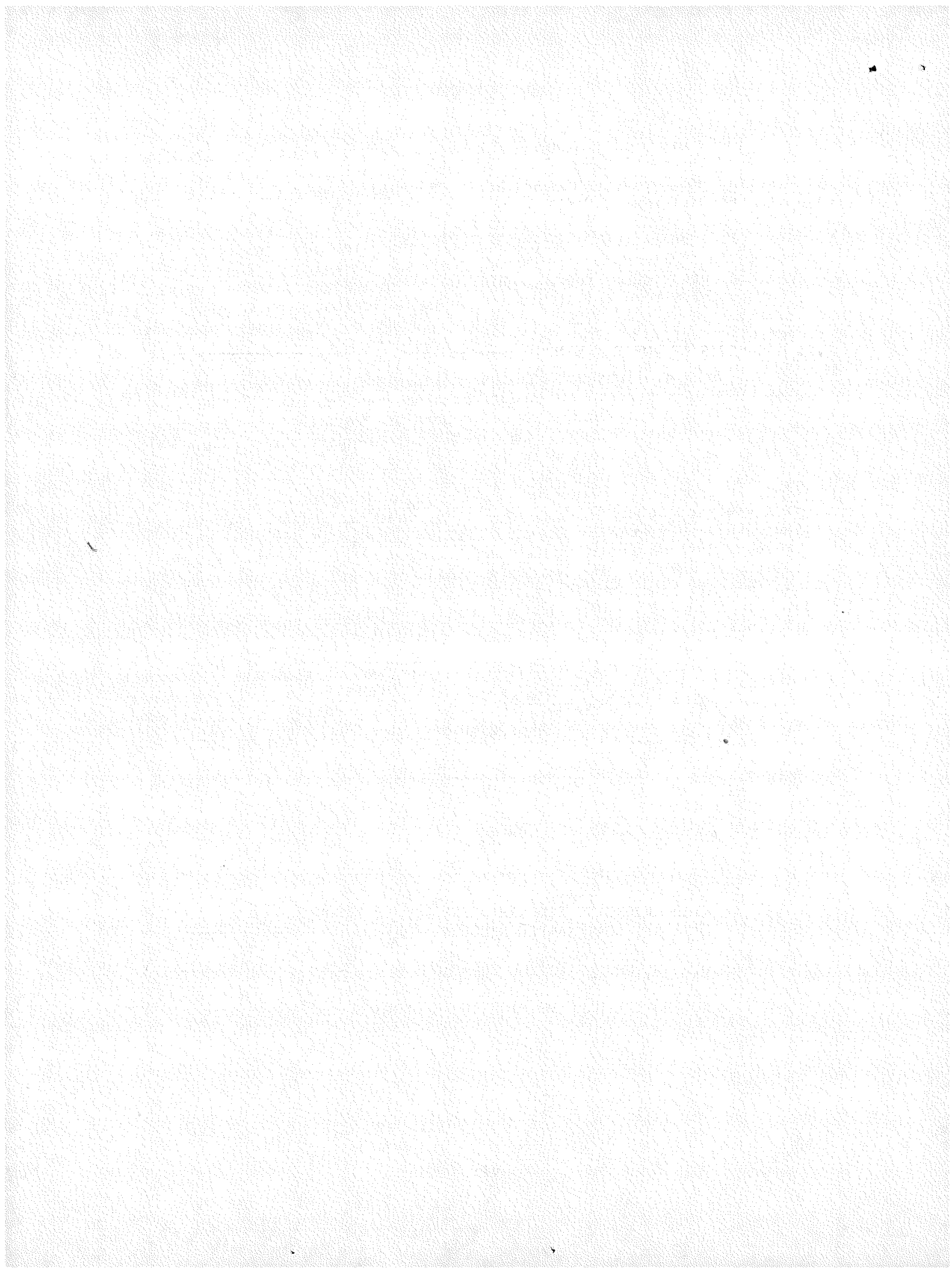
This document describes the objectives, approach, and FY'78 progress and results of the Aerodynamic Resistance Reduction work element of the Electric and Hybrid Vehicle System R&D Project managed by JPL for the Department of Energy.

The generation of an EVH aerodynamic data base was initiated by conducting full-scale wind tunnel tests on 16 vehicles. Zero-yaw drag coefficients ranged from a high of 0.58 for a boxy delivery van and an open roadster to a low of about 0.34 for a current 4-passenger prototype automobile which was designed with aerodynamics as an integrated parameter.

A subscale investigation was performed in order to identify any characteristic effects of aspect ratio or fineness ratio which might appear if electric vehicle shape proportions were to vary significantly from current automobiles. Some preliminary results are presented which indicate a 5-10% variation in drag over the range of interest.

A rigorous procedure was developed in order to determine effective drag coefficient wind-weighting factors over J227a driving cycles in the presence of annual mean wind fields. The application of this procedure allows a user to accurately account for statistical wind effects in computer simulations by means of a modified constant-drag coefficient. Such coefficients, when properly weighted, were found to be from 5 to 65% greater than the zero-yaw drag coefficient in the cases presented.

In order to guide preliminary design work, a review of the general principles of the aerodynamic design of automobiles is presented along with several drag-estimating procedures and commentary. Also included is a vehicle aerodynamics bibliography of over 160 entries, in six general categories.



## CONTENTS

I.	INTRODUCTION -----	1
II.	OBJECTIVES AND APPROACH -----	5
III.	AERODYNAMIC DATA BASE -----	7
IV.	ROAD TEST DATA CORRELATION -----	13
V.	SUBSCALE SHAPE PARAMETER INVESTIGATION -----	15
VI.	EFFECTS OF AMBIENT WINDS -----	21
VII.	GENERAL AERODYNAMIC DESIGN PRINCIPLES -----	25
A.	SOURCES OF DRAG -----	25
B.	DRAG ESTIMATION METHODS -----	27
	BIBLIOGRAPHY -----	35
A.	GENERAL AERODYNAMICS -----	35
B.	FACILITY TESTING -----	40
C.	ROAD TESTING -----	42
D.	NOISE -----	44
E.	STABILITY AND HANDLING -----	44
F.	GENERAL, BOOKS, PROCEEDINGS -----	45
	REFERENCES -----	47

## APPENDIXES

A.	EHV SOURCE LIST -----	A-1
B.	WIND-WEIGHTING PROGRAM (EHVSCD): (1) SOURCE LISTING, (2) EXAMPLE RESULTS -----	B-1
C.	WIND-WEIGHTING FACTOR EQUATIONS -----	C-1
D.	AUTOMOTIVE DRAG PREDICTION PROCEDURES -----	D-1

## Figures

1.	Road Energy Component Split Over the SAE J227a D Driving Cycle (No Regenerative Braking) -----	2
2.	Projected Vehicle Range Over the SAE J227a D Cycle as a Function of Various Parameters (No Regenerative Braking) -----	2
3.	Vehicles Tested in Lockheed-Georgia's Low-Speed Wind Tunnel -----	8
4.	Basic Sharp-Edged Model Mounted in GALCIT Wind Tunnel -----	16
5.	Basic Round-Edged Model Mounted in GALCIT Wind Tunnel -----	16
6.	Some of the 56 Pieces Used to Alter Aspect and Fineness Ratios -----	17
7.	Drag Coefficient vs. Fineness Ratio for Sharp- and Rounded-Edged Automobile Shapes (Ground Clearance = 15% of Body Width) -----	17
8.	Drag vs. Ground Clearance; Aspect Ratio = 0.88 -----	18
9.	Drag vs. Aspect Ratio at Two Ground Clearances -----	19
10.	Drag vs. Fineness Ratio at Two Ground Clearances -----	19
11.	SAE J227a Electric Vehicle Test Cycles -----	22
12.	Annual Wind Speed Duration Curves - Probability of Occurrence -----	22
13.	Aerodynamic Drag Coefficient as a Function of Yaw Angle (Parametric Variations Used in the Analysis) -----	23
14.	Distribution of IC Engine Vehicle Aerodynamic Drag -----	28

Tables

1.	Data Base Vehicles -----	10
2.	Zero Yaw Drag Coefficient and Frontal Area of Several Electric and Hybrid Subcompact IC Engine Vehicles - Windows Closed and Radiator Blocked -----	10
3.	Wind-Weighting Factors of Example Cases -----	24
4.	Drag Increment Generalizations -----	32

## SECTION I

### INTRODUCTION

As an automobile moves along a road surface, the resulting displacement of the air gives rise to various forces and moments. Computer simulations have demonstrated that, under some atmospheric and operating conditions (or driving cycles), these forces and moments can be of significant magnitude. Tire/road forces are normally a weak linear function of velocity in the range of interest. Aerodynamic forces increase with the square of the velocity; hence the power required to overcome aerodynamic resistance increases as the cube of the car's velocity. It is therefore imperative that proper attention be paid to aerodynamic design.

Minimization of drag is not the only factor involved in optimizing aerodynamic efficiency. Others include:

- (1) Lift distribution and side wind stability.
- (2) Ventilation of occupants, motor, batteries, etc.
- (3) Splash or road dirt accumulation.
- (4) Interior noise level.

These, however, will not be given further attention at this time, since it is drag that principally affects driving range.

The aerodynamic drag component clearly dominates the road load requirement at high cruise speeds. It is important to note, however, that even over an SAE J227a D cycle (maximum speed only 72 kph), more than 35% of the energy (at the road-wheel interface) goes to overcome aerodynamic drag for a typical subcompact class electric vehicle with no regenerative braking (see Figure 1). (The addition of regenerative braking could increase the relative aerodynamic contribution to almost 40% in this case.) The rolling component (1.4% of the vehicle weight at zero speed) includes all internal losses from tires, gears, etc.

It is reasonable to expect that, with vigorous design efforts, a drag area ( $C_D A$ )\* of  $0.54 \text{ m}^2$  ( $5.8 \text{ ft}^2$ ) may be achievable — a 40% reduction from  $0.9 \text{ m}^2$  ( $9.7 \text{ ft}^2$ ), which is typical of today's subcompact car. As Figure 2 shows, this could result in a 20% increase in the SAE J227a D cycle range. To achieve a similar benefit via a reduction in rolling

---

\* The drag coefficient,  $C_D$ , is nondimensional and is defined as

$$C_D = \text{Drag Force} / (1/2 \times \text{Air Density} \times \text{Velocity}^2 \times \text{Frontal Area})$$

The frontal area,  $A$ , is the vehicle's projected frontal area including tires but excluding appendages such as mirrors, roof racks, antennas, etc.

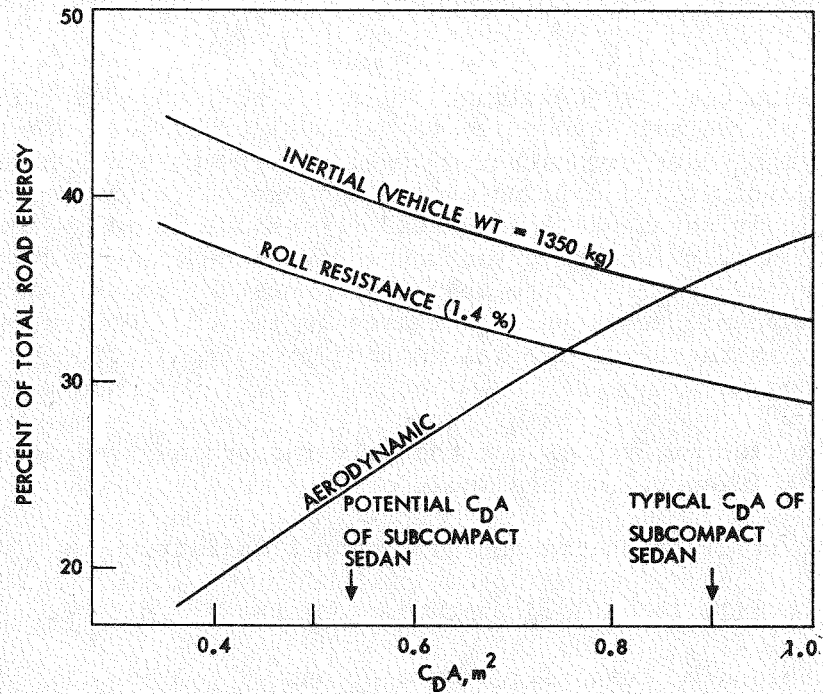


Figure 1. Road Energy Component Split Over the SAE J227a D Driving Cycle (No Regenerative Braking)

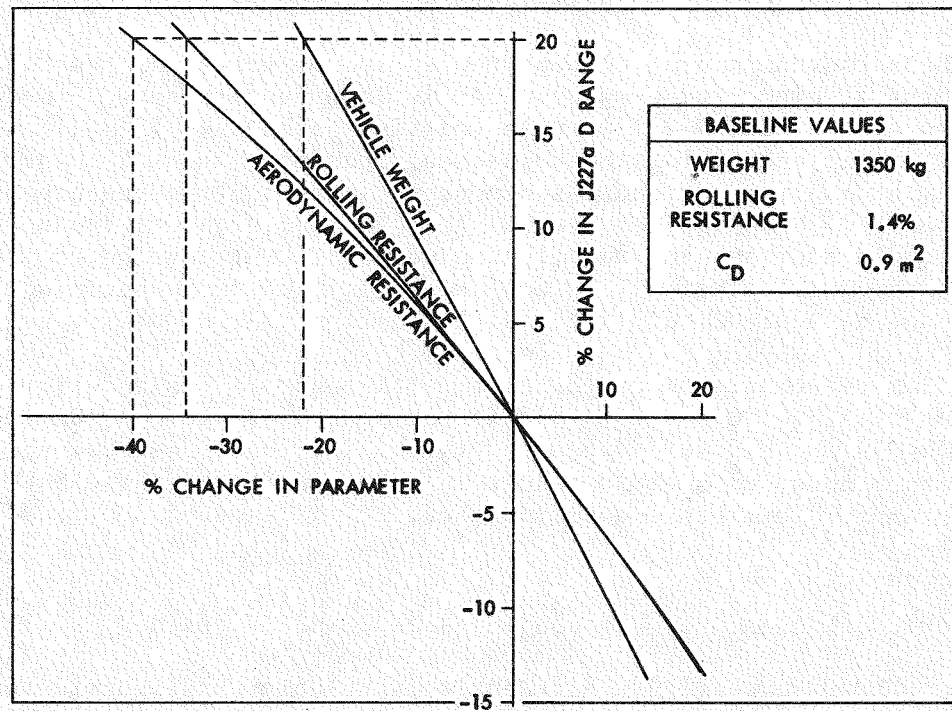
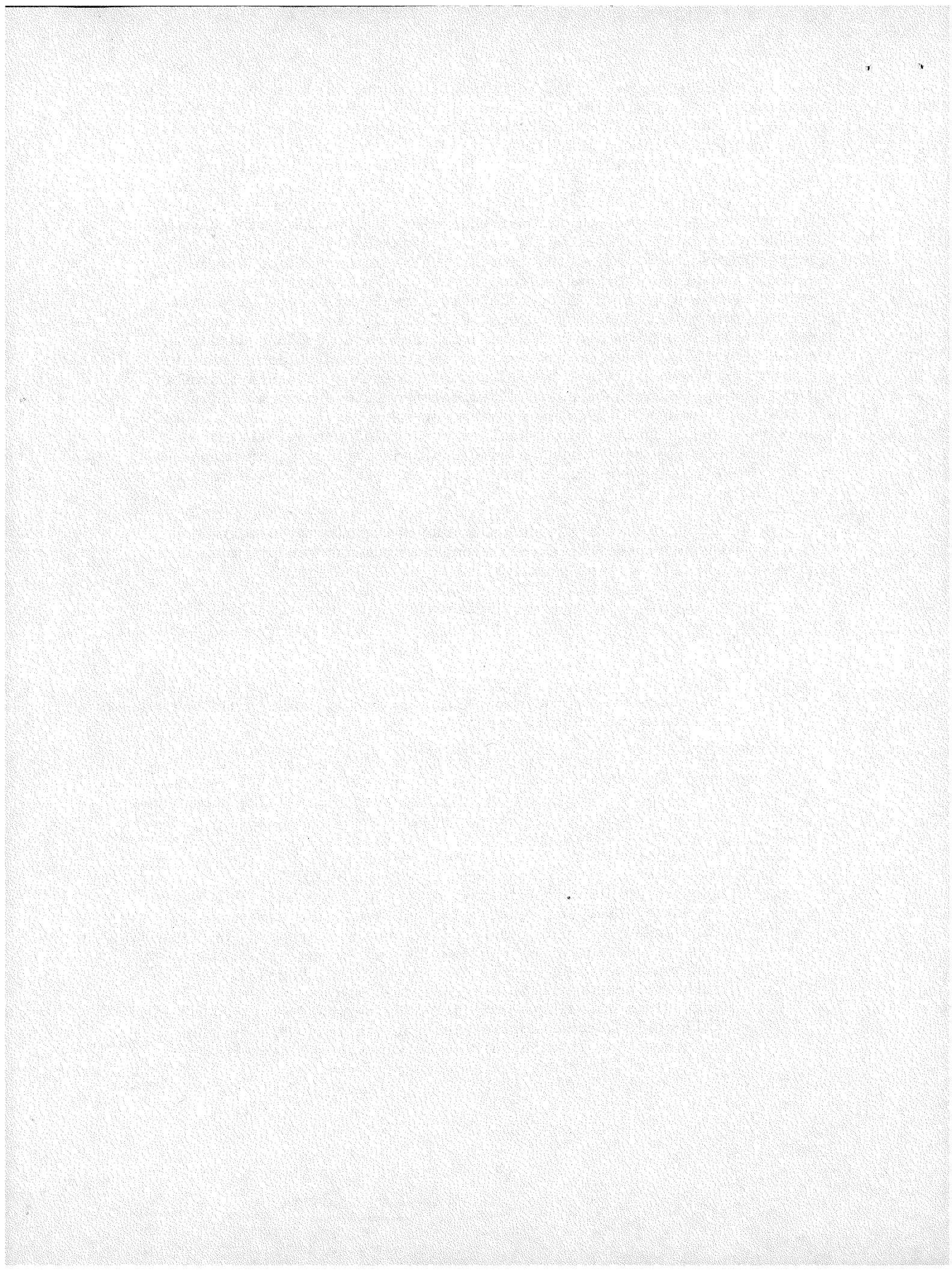


Figure 2. Projected Vehicle Range Over the SAE J227a D Cycle as a Function of Various Parameters (No Regenerative Braking)

resistance would require a 34% reduction, to about 0.9% (a rather unrealistic value since this includes all rolling losses in addition to that due to the tires), or a 22% reduction in vehicle weight (300 kg). These examples, although simplified, tend to demonstrate the potential benefits from, and justification for pursuing aerodynamic resistance reduction.

It should also be pointed out that electric vehicles (EV) have certain inherent attributes which are aerodynamically beneficial. Internal aerodynamic losses associated with radiator airflow for an internal combustion (IC) engine counterpart are not a factor for electric vehicles (EVs). Also, full belly pans, which have given rise to safety and maintenance objections in IC engine cars, may be quite acceptable in an EV. These two considerations alone could reduce the drag of an EV by as much as 20% over an IC engine equivalent. Further, the requirements for battery volume and placement may dictate ranges of body proportions which are quite different from those of conventional automobiles. Center longitudinal battery tunnels, for instance, cause a vehicle to be unusually wide; smaller motors and potentially more compact drive lines may allow a significant redistribution of proportions. These could have either beneficial or detrimental aerodynamic consequences.

This report examines several elements pertaining to electric vehicle aerodynamic resistance reduction and presents the program results for the 1978 fiscal year.



## SECTION II

### OBJECTIVES AND APPROACH

The general objective of this investigation is to provide trade-off information to industry to aid in the development of aerodynamically efficient electric and hybrid vehicles, and specifically, to develop simplified aerodynamic design principles and procedures suitable for use by the EHV industry. This does not imply that a generalized "hand-book" approach to aerodynamic design will be developed during this program; however, the utility and limitations of such generalizations will be examined. Though elementary pitfalls can sensibly be avoided by using such an approach, it is believed that an optimized design can be realized only through an extensive experimental wind tunnel development program. Subscale developmental testing can yield valuable relative trade-off information; full-scale testing may be required to determine absolute levels.

The approach adopted for this work element includes the following steps:

- (1) Assess the state of the art. More than 20 individuals in government, private industry and academic institutions were contacted. Discussions centered on the general state-of-the-art of automotive aerodynamics status and the special characteristics of electric vehicles. Automobiles are characterized as aerodynamically bluff bodies operating in a ground effect with large regions of separated flow. As such, analysis is usually not amenable to classical theoretical treatment and is therefore (currently) an empirical process. A bibliography covering a wide range of automotive aerodynamic subjects has been collected and is contained in this report.
- (2) Assemble a realistic aerodynamic data base for representative electric vehicles. For proprietary and other reasons, there is a great lack of reliable aerodynamic data on full scale IC engine vehicles. There is even less data available for electric vehicles, which tend to differ from conventional vehicles in air inlet size, underbody design, and dimensional proportions. In order to provide the necessary support to the EHV industry, an aerodynamic data base must be established and continually updated. The data base is to be used to guide the formulation of engineering design concepts in the areas of reducing aerodynamic drag, improving ventilation and cooling, and providing more accurate input to computer simulation studies and dynamometer testing. This is being accomplished by assembling what limited full-scale data on applicable vehicles is available, and supplementing it with full-scale wind tunnel test results on electric, hybrid, and subcompact cars.

- (3) Investigate the aerodynamic effects of systematic variations in dimensional proportions. Some electric and hybrid vehicles are now being designed from the ground up, rather than as conversions of conventional heat-engine cars. The aerodynamic design principles employed in the past may not be directly applicable owing to fundamental differences in the design. For instance, the effects of aspect ratio (height/width) and fineness ratio (length/effective diameter) for automobiles are not sufficiently well understood to allow preliminary design trade-offs between component placement and aerodynamic consequences to be made. For these reasons, subscale wind tunnel tests on a simplified automobile shape were performed.
- (4) Relate the aerodynamic results from various test techniques. To establish absolute levels of drag and rolling resistance under road conditions, some of the vehicles tested at full-scale in the wind tunnel will be road tested using the coast-down technique. This is particularly important for electric vehicles since drag reduction strategies may include full or partial underpanning and wind tunnel testing alone may not produce conclusive information. This procedure, supplemented by wind tunnel yaw data, will provide the complete information required for detailed cycle simulations and range calculations. In addition, wherever available, subscale wind tunnel data can be compared to full-scale data in order to develop correlation and confidence levels.
- (5) Investigate the effects of ambient winds on aerodynamic drag. Since a road vehicle, statistically, operates in a windy environment, a rational wind-weighting procedure must be used to determine the effective drag level. Several procedures have been developed around "statistical" winds (References 1 and 2), but these do not superimpose a driving cycle. This is a necessary extension in order to properly simulate the aerodynamic contribution in computer and dynamometer simulations.

### SECTION III

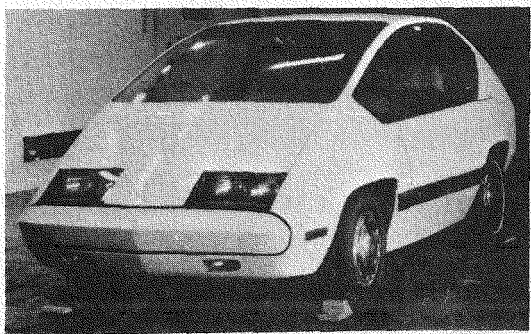
#### AERODYNAMIC DATA BASE

As mentioned earlier, very little reliable aerodynamic data on conventional automobiles, is available, and virtually none on special electric or hybrid vehicles. The automobile manufacturers, both foreign and domestic, have generated a great deal of aerodynamic information for IC engine vehicles, but it remains largely proprietary. Most of the data that is available is from subscale wind tunnel tests of questionable or unknown origin. Herein lies a basic problem with random wind tunnel data: it is generally not directly comparable. Owing to such factors as scale, level of detail (internal flow paths, undercarriage, etc.), flow conditions, and data reduction procedures, the absolute values of the coefficients are of limited value. The difference in measured drag between a "reasonably detailed" scale model and the full-sized production vehicle is often 20% or greater. The same automobile tested in two different tunnels may yield drag results which differ by 10%. The magnitude of various wall corrections alone can modify the drag by 10%. To maximize its usefulness, a data base should be generated at the same model scale, in the same tunnel, under the same conditions, and be handled using identical data reduction procedures. The relative effects represented by the data base should then be sufficiently reliable. Correlations with road test results can help to establish a confidence level for the absolute values.

With this background in mind, it was determined that the development of an EHV aerodynamic data base should be initiated by performing full-scale tests in the Lockheed-Georgia low-speed wind tunnel. A Request for Quotation (RFQ) was prepared and sent to 25 possible owners or developers of electric or hybrid vehicles asking for the use of a vehicle for aerodynamic characterization testing during a specific time period. This source list is presented in Appendix A. Nine bids were received before the RFQ closing date. Among the selection criteria used were

- (1) Availability.
- (2) Compatibility with wind tunnel balance system.
- (3) Aerodynamic interest.
- (4) Loan and transportation fees.

Four vehicles were selected by this process. In addition, three electric vehicles were loaned by the NASA's Lewis Research Center. To supplement the group, several conventional IC subcompacts were borrowed from local dealerships and individuals. In two cases, a facsimile of an IC engine/EHV conversion was substituted. The vehicles tested in this group are shown in Figure 3 and are listed in Table 1.



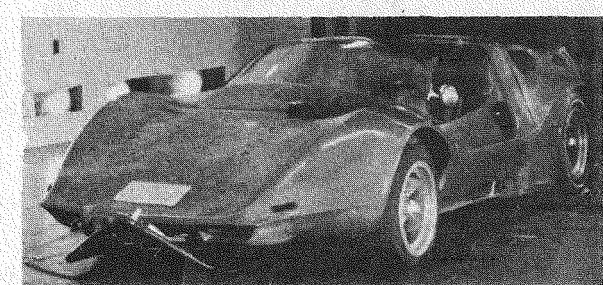
a. CDA Town Car



b. Centennial Electric



c. HEVAN



d. Kaylor GT



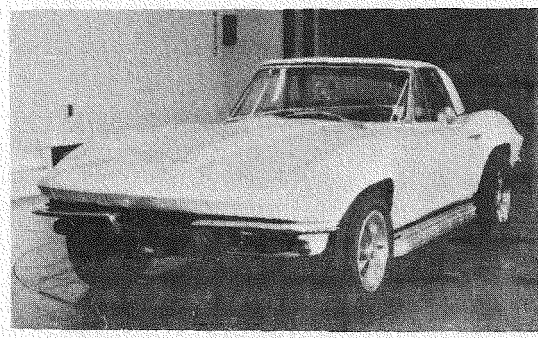
e. Citicar



f. Elcar



g. Otis Van



h. '67 Corvette

Figure 3. Vehicles Tested in Lockheed-Georgia's Low-Speed Wind Tunnel



i. Delta 88 Gemini II



j. Pacer Sedan



k. Pacer Wagon



l. Honda Sedan



m. Honda Wagon



n. Fiesta



o. Horizon



p. Chevette

Figure 3. Vehicles Tested in Lockheed-Georgia's Low-Speed Wind Tunnel  
(cont'd)

Table 1. Data Base Vehicles

Figure	Vehicle	Type
3a	Copper Development Association: Town Car	2-passenger electric commuter
3b	General Electric Co.: Centennial Electric	4-passenger electric commuter
3c	Energy Research and Development Corp.: HEVAN	Hybrid-electric delivery van
3d	Kaylor Energy Products: Kaylor GT	2-passenger hybrid-electric open roadster
3e	Sebring-Vanguard <sup>1</sup> : Citicar	2-passenger electric commuter
3f	Zagato-Elcar Corp. <sup>1</sup> : Elcar	2-passenger electric commuter
3g	Otis Elevator Co. <sup>1</sup> : Otis P 500 A Van	Electric delivery van
3h	GM Corp.: 1967 Chevrolet Corvette	Internal combustion engine (ICE) <sup>2</sup>
3i	GM Corp.: 1978 Oldsmobile Delta 88	ICE <sup>3</sup>
3j	American Motors Corp.: 1978 Pacer Sedan	ICE
3k	American Motors Corp.: Pacer Station Wagon	ICE
3l	Honda Motors: 1978 Civic Sedan	ICE
3m	Honda Motors: 1978 Civic Wagon	ICE
3n	Ford Motor Co.: 1978 Fiesta	ICE
3o	Chrysler Corp.: 1978 Plymouth Horizon	ICE
3p	GM Corp.: 1978 Chevrolet Chevette	ICE

<sup>1</sup>Loaned by NASA-Lewis Research Center, Cleveland, OH.

<sup>2</sup>This production IC engine Corvette represented a reasonable facsimile of the Cutler-Hammer Electric '67 Corvette of Santini. The front grille was blocked in order to eliminate the radiator losses, which are not present in the electric version.

<sup>3</sup>This production IC engine Delta 88 was a reasonable facsimile of the National Motors Hybrid-Electric Gemini II. Here the radiator was not blocked since the hybrid vehicle retains its V-6 engine and cooling system.

The vehicles were mounted on the external balance by means of a four-point support system. No attachment was required; the wheels merely rested on the four pads with the parking brakes locked. The friction between the tires and the pads was normally sufficient to maintain model position. In certain cases, chocks were placed behind the tires. Because of the extremely short wheelbases of some of these electric vehicles, it was necessary to use pad extensions. These raised the position of the vehicle in the tunnel by approximately 3 centimeters. To quantify the effect of this position change, tests were made using spacers with a few of the vehicles that were capable of using the unmodified pads. Elevating a vehicle in this manner appeared to increase the measured drag by 1-2% over the entire yaw range.

All tests were performed at 88 kph and the yaw angle ( $\psi$ ) was varied through  $\pm 40$  degrees. Runs were also made on all vehicles with the two front windows open. Some tests of IC engine cars were run with radiators both open and blocked.

The preliminary drag results are shown in Table 2. A complete data report on these tests will be issued under separate cover during FY 79. However, it is interesting to note that the selected vehicles represent a range of zero-yaw drag coefficients from 0.337 to 0.583. Further, the highest value (least aerodynamically efficient) of the group was the Kaylor open roadster followed closely by the boxey Otis van; however, the HEVAN drag coefficient was nearly 15% less at 0.497 despite its boxey lines. Another interesting result was that the Horizon's drag coefficient was over 18% lower than the Chevette's even though they are very similar in shape\*. Both the Copper Development Association's Town Car and General Electric's Centennial have drag values significantly lower than the rest of the group — a probable result of the importance of aerodynamics in the design theme and sub-scale wind tunnel testing.

---

\* The relative drag levels of the cars tested in the Lockheed-Georgia wind tunnel must not be taken as typical of all their manufacturer's products.

Table 2. Zero Yaw Drag Coefficient and Frontal Area of Several Electric Hybrid and Subcompact IC Engine Vehicles - Windows Closed and Radiators Blocked Where Appropriate\*

Vehicle	$C_{D_0}$	$A, m^2$
CDA Town Car	0.367	1.754
GE Centennial	0.337	1.851
Energy R&D HEVAN	0.497	3.283
Kaylor GT	0.583	1.359
Citicar	0.541	1.700
Elcar	0.490	1.838
Otis Van	0.581	2.593
Corvette	0.490	1.925
Delta 88	0.558	2.077
Pacer Sedan	0.450	2.222
Pacer Wagon	0.406	2.225
Honda Sedan	0.503	1.630
Honda Wagon	0.514	1.685
Ford Fiesta	0.468	1.747
Plymouth Horizon	0.411	1.906
Chevrolet Chevette	0.502	1.765

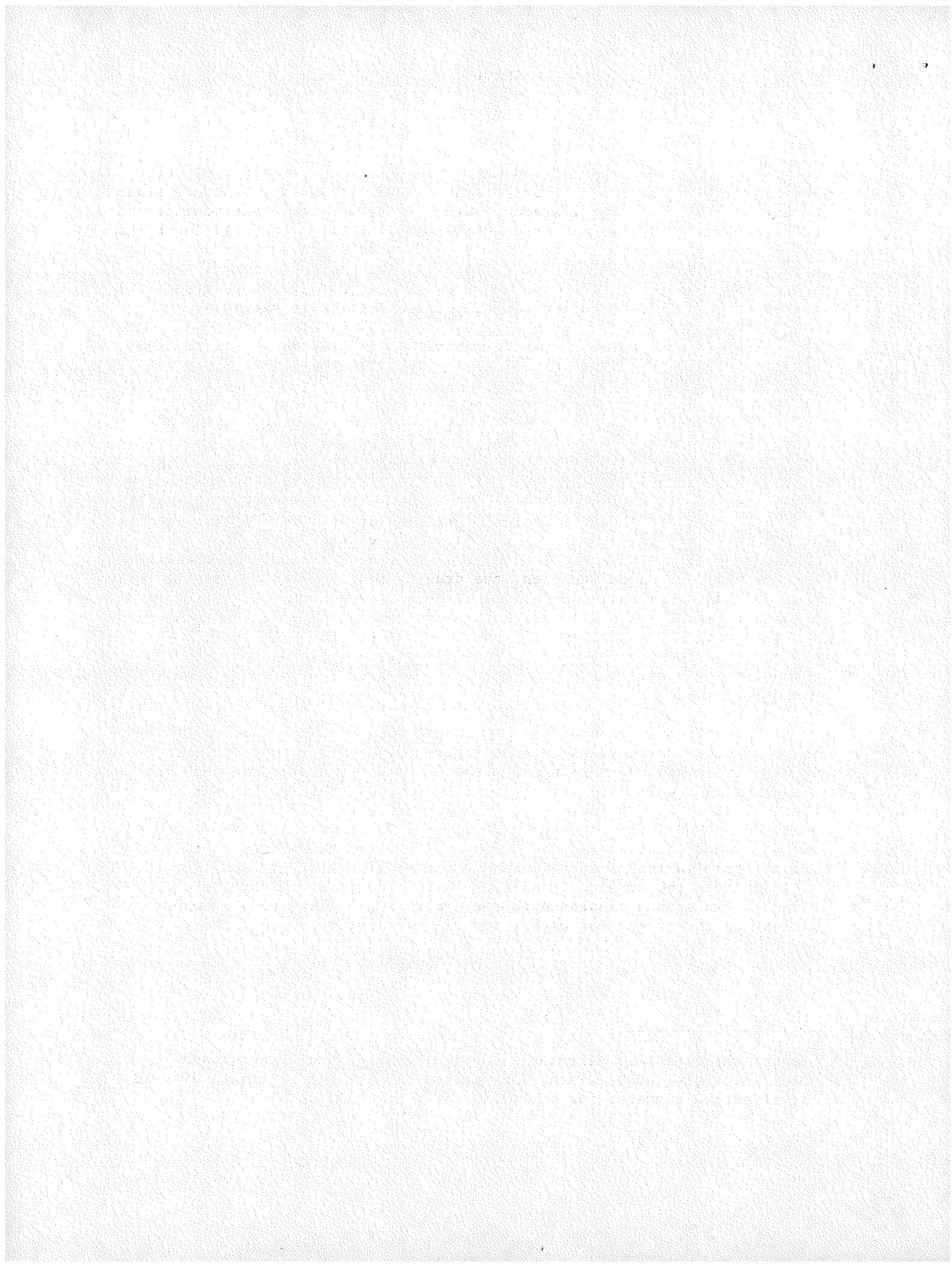
\*All IC engine vehicles had their grilles covered since an electric version would not have a radiator airflow requirement and the resulting drag. The Oldsmobile Delta 88, however, represented the National Motors Gemini II parallel hybrid vehicle, which retains the standard cooling system.

## SECTION IV

### ROAD TEST DATA CORRELATION

Since the vehicle/road interface is not precisely modeled in a wind tunnel, there is often speculation concerning the accuracy of the results. Actual road test drag determination may be preferred in principle, but it is extremely difficult to accomplish in practice; also, it is not practical to systematically investigate yaw effects. However, certain single point correlations can and should be made. Earlier investigations (Reference 3) determined that, for a 1975 Chevrolet Impala, there was essentially a one-to-one correlation between drag values from wind tunnel and properly conducted coast-down test results. It was speculated that this result was perhaps fortuitous and may be a function of shape or configuration.

Consequently, in the course of this project, coast-down tests are planned for the HEVAN (vehicle No. 3, Table 1), the Kaylor GT (vehicle No. 4) and the Cutler-Hammer Electric '67 Corvette (vehicle No. 8 is a reasonable facsimile). Unfortunately, no final results from the coast-down testing were available for presentation in this report; these will be presented as part of a comprehensive report on this data base testing to be issued during FY'79.



## SECTION V

### SUBSCALE SHAPE PARAMETER INVESTIGATION

Because of their special battery packaging requirements, electric vehicles may not be subject to the same design constraints as conventional IC engine vehicles. For instance, owing to the use of a central battery tunnel, a small vehicle may be unusually wide or long. A series of tests was therefore performed in the GALCIT 10-foot wind tunnel (Caltech) to determine if aspect ratio or fineness ratio\* was an important aerodynamic parameter, and further, whether one can generalize the effect of either or both in combination for simplified automobile shapes.

These tests were exploratory in nature, to determine what, if any, trends would appear. The initial tests involved both a sharp-edged and a round-edged basic model (Figures 4 and 5), in order to quantify the effect of local flow separation on the observed aerodynamic trends.

The parameters varied were height, length, width, and ground clearance; Figure 6 illustrates the model construction technique. Three variations were available for each of the four parameters. It was not often possible to keep one parameter constant while independently varying each of the others. Figure 7 illustrates the drag trends demonstrated by highly separated (sharp-edged model) and highly attached (round-edged model) flow situations at low to moderate fineness ratios. As one might expect, for very short vehicles, the drag is reduced with increasing fineness ratio. This is probably due to a reduction in the form drag component (see Section VII) at the expense of a small increase in surface friction drag. Owing to local separation points, the drag gradient is not as large for the sharp-edged model as for the round-edged, but the trend is not significantly different. Subsequent tests involved only the round-edged model.

The effects of ground clearance were found to be significant with these smooth-underbody models (see Figure 8). This also presents a problem in data presentation since the manner by which the ground clearance is nondimensionalized can distort the effects of aspect and fineness ratios. For instance, if the ground clearance is nondimensionalized by body width and the aspect ratio is varied by changes in body width, ground clearance changes with aspect ratio and dominates the whole effect. Similarly, ground clearance nondimensionalized by body length will dominate the effects of changes in fineness ratio. For these reasons, two ground clearance parameters,  $g/L$  and  $g/W$ , are used when evaluating the effects of aspect and fineness ratios, respectively.

---

\* Aspect ratio (AR) is defined as body height (not including ground clearance) divided by width, and fineness ratio (FR) as length divided by effective diameter (or equivalent area circle).

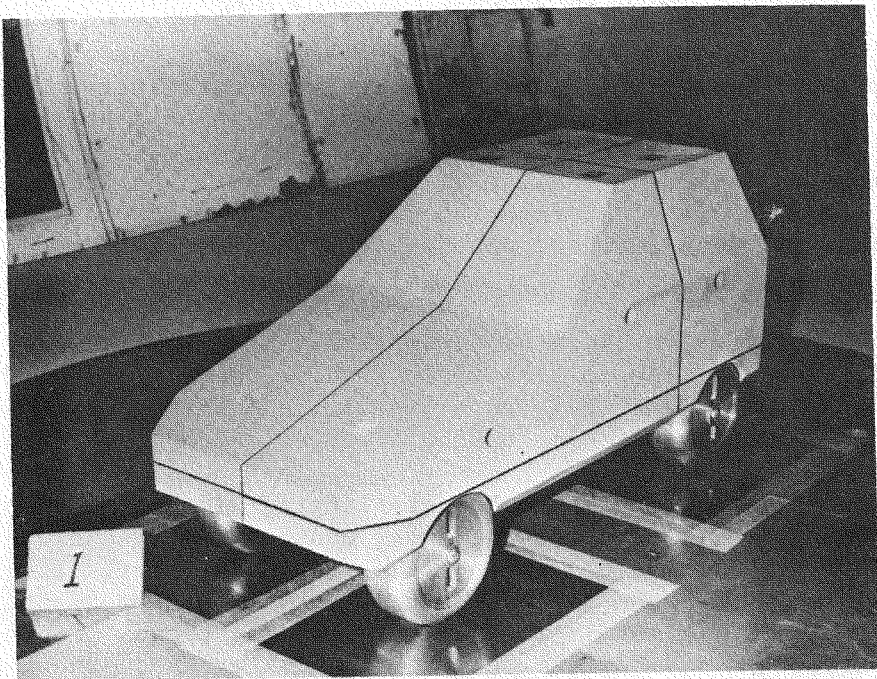


Figure 4. Basic Sharp-Edged Model Mounted in GALCIT Wind Tunnel

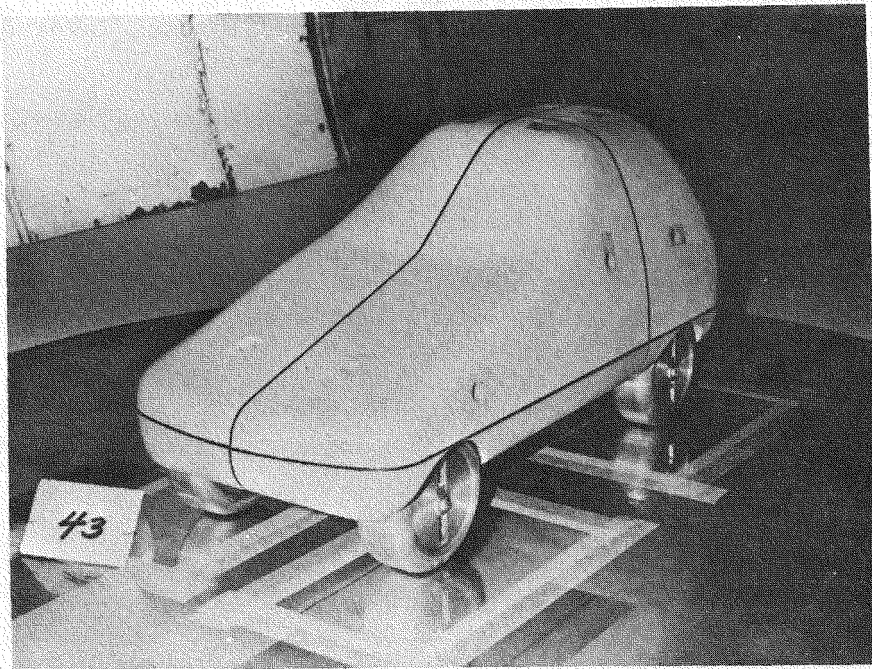


Figure 5. Basic Round-Edged Model Mounted in GALCIT Wind Tunnel

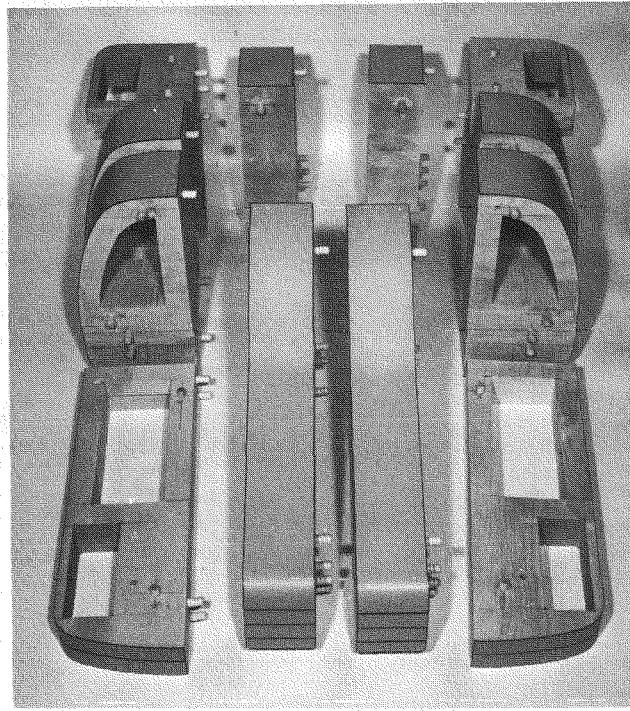


Figure 6. Some of the 56 Pieces Used to Alter Aspect and Fineness Ratios

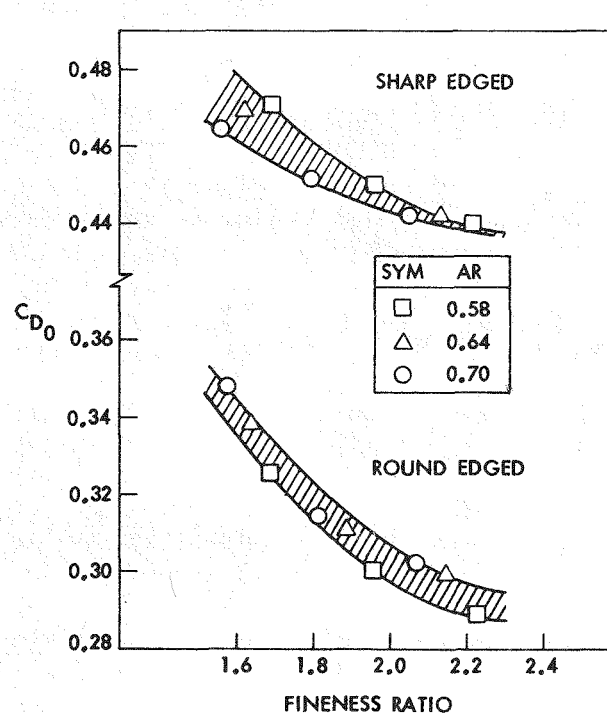


Figure 7. Drag Coefficient vs. Fineness Ratio for Sharp-Edged and Round-Edged Automobile Shapes (Ground Clearance = 15% of Body Width)

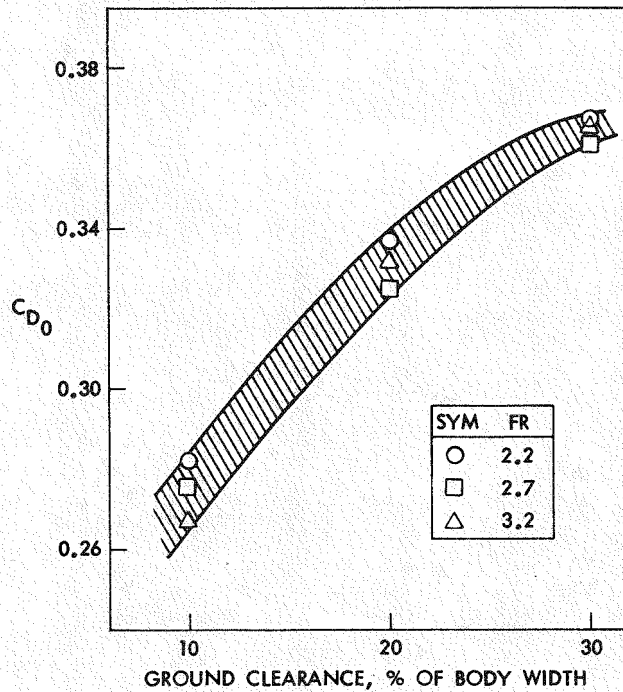


Figure 8. Drag vs. Ground Clearance.  
Aspect Ratio = 0.88

The effect of aspect ratio on drag is shown in Figure 9 at two levels of ground clearance representative of present day automobiles ( $g/L = 5\%$ ) and vans ( $g/L = 8\%$ ). In both cases, the drag usually increases with aspect ratio (short and wide has some advantages over tall and narrow), being more pronounced at the highest fineness ratio (longest vehicle). For high-ground-clearance vehicles, there seems to be a weak aspect ratio effect up to about  $AR = 0.8$ ; beyond that point, the drag increases significantly. This situation may help to explain why the Otis van (Figure 3g) with an aspect ratio of 1.1 had a drag coefficient 16% higher (Table 2) than the HEVAN (Figure 3c) with an aspect ratio of 0.85. Although certain shape and position factors were dissimilar, the relative drag difference may be explained in part by the difference in aspect ratios.

The effect of fineness ratio (Figure 10) is a little more confusing in that the trends with constant aspect ratios are not as internally consistent. Note also, that the two ground clearances representing "automotive ( $g/W = 10\%$ ) and van-like ( $g/W = 20\%$ )" are nondimensionalized by body width for the reasons explained earlier. In general, the trend is consistent with Figure 7 which covered the very low fineness-ratio end of the spectrum. However, as the fineness ratio is increased, significant drag reduction ceases and the drag actually begins to increase beyond a fineness ratio of 2.7 at the higher ground clearance. This may indeed be the result of a rapid buildup of the surface friction drag component (see Section VII), which may be magnified in the underbody region at high ground clearances.

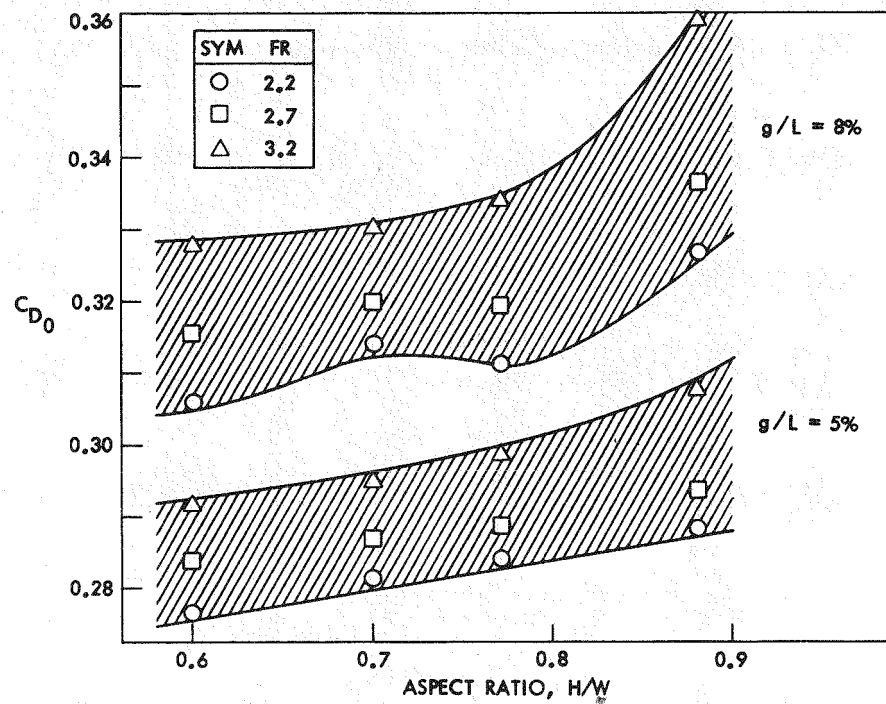


Figure 9. Drag vs. Aspect Ratio at Two Ground Clearances

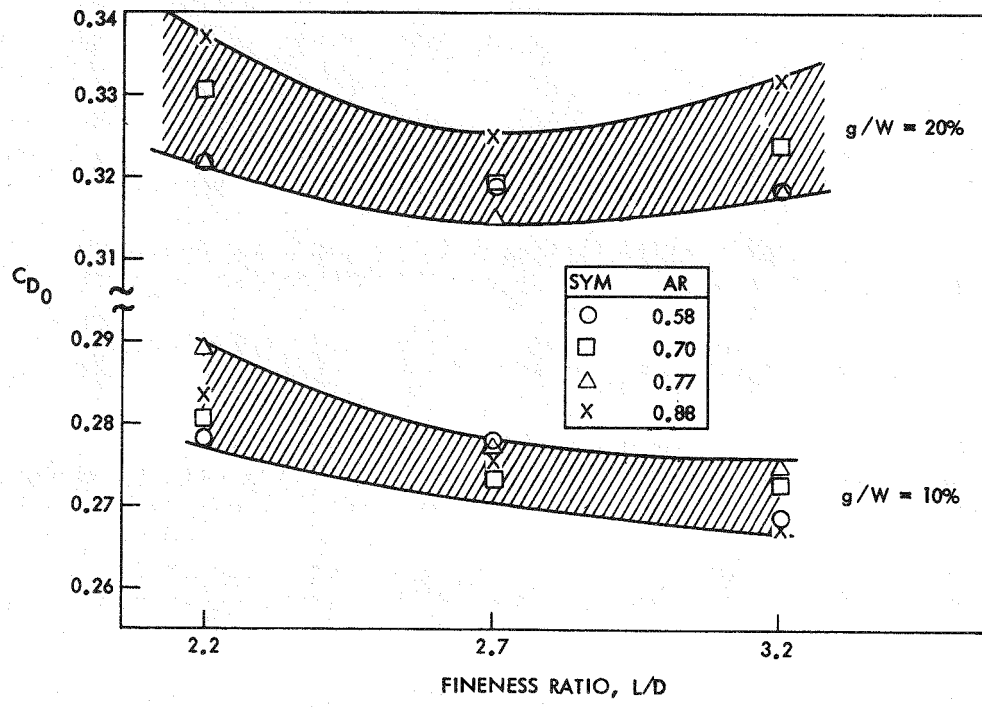


Figure 10. Drag vs. Fineness Ratio at Two Ground Clearances

In summary, these results indicate that there are aspect and fineness ratio effects on vehicle drag that warrant consideration during initial design stages when packaging requirements are being developed. More data are required to fill the gaps and extend the results.

## SECTION VI

### EFFECTS OF AMBIENT WINDS

As a vehicle moves along a roadway, it normally operates in a windy environment. Since the resulting wind vector is usually not aligned with the vehicle's longitudinal axis, it is effectively yawed with respect to the flow. Therefore, range predictions that use zero-yaw drag values will inaccurately characterize the aerodynamic contribution. For a vehicle operating over a prescribed driving cycle, a statistically modeled wind vector can be superimposed, yielding an instantaneous yaw angle. If the functional dependence of drag coefficient on yaw angle is known, the effective instantaneous aerodynamic resistance can be calculated, and the effective drag coefficient factor over the cycle can be established. That is, the constant-drag coefficient used in vehicle computer simulators need only be modified by this factor to rigorously account for the effects of statistical ambient winds.

Initially, this procedure was developed around the EPA urban and highway cycles for IC engine vehicles (References 4, 5, and 6). Since then, cycles specifically for EHV evaluation (SAE J227a), have been developed, and the procedure has been modified for electrics. This modified program is called EHVSCD (Electric Hybrid Vehicle System C D where C D refers to the aerodynamic drag coefficient,  $C_D$ ). This program is shown in its entirety in Appendix B along with a printout for an example case.

The approach taken is to figuratively drive a vehicle over a prescribed velocity-time schedule in the presence of a statistically varying wind which is equally probable from any direction. The resultant combination of the vehicle and wind vectors yields an instantaneous yaw angle with respect to the vehicle. If the vehicle's drag-yaw characteristic is known, the resultant drag may be determined at each instant. Therefore, the energy required to overcome aerodynamic resistance is calculated by integrating the instantaneous aerodynamic power required over the cycle. It is then possible to determine what constant drag coefficient would be necessary in order to yield the same result. The ratio of this new effective coefficient,  $C_{D_{eff}}$ , to the original zero-yaw drag coefficient ( $C_{D_0}$ ) is the wind-weighting factor,  $F$ .  $F$  is thus a multiplier to correct the zero-yaw coefficient for ambient winds in computer simulations.

Factors have been developed for the SAE J227a B, C, and D cycles (Figure 11), two annual mean wind speed (AMWS) probability functions (Figure 12), and three drag-coefficient vs. yaw-angle characteristic curves (Figure 13). Reference 6 determined that the shape of these yaw curves beyond about 40 degrees was of second-order importance. The drag coefficient usually reaches a maximum between 20 and 40 degrees and, for

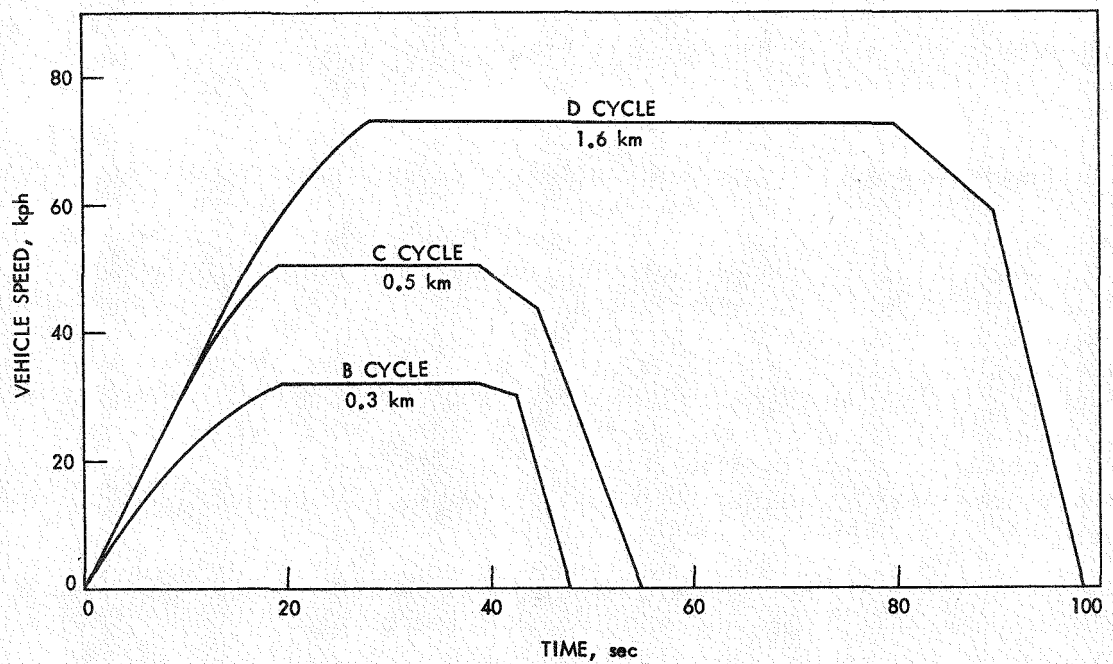


Figure 11. SAE J227a Electric Vehicle Test Cycles

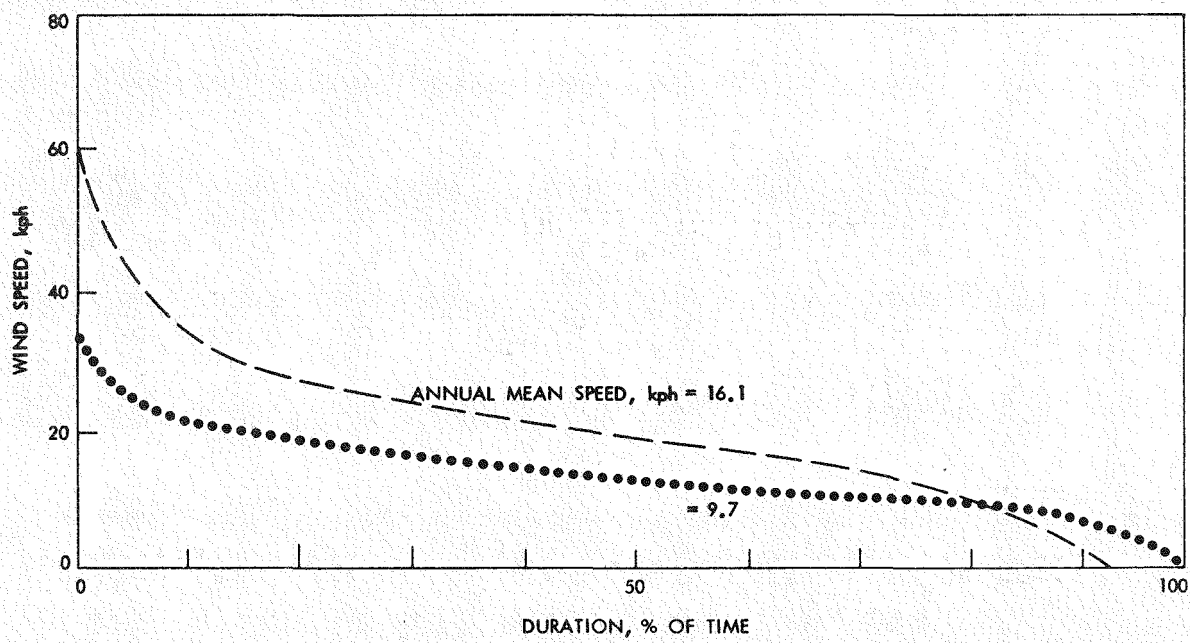


Figure 12. Annual Wind Speed Duration Curves -- Probability of Occurrence

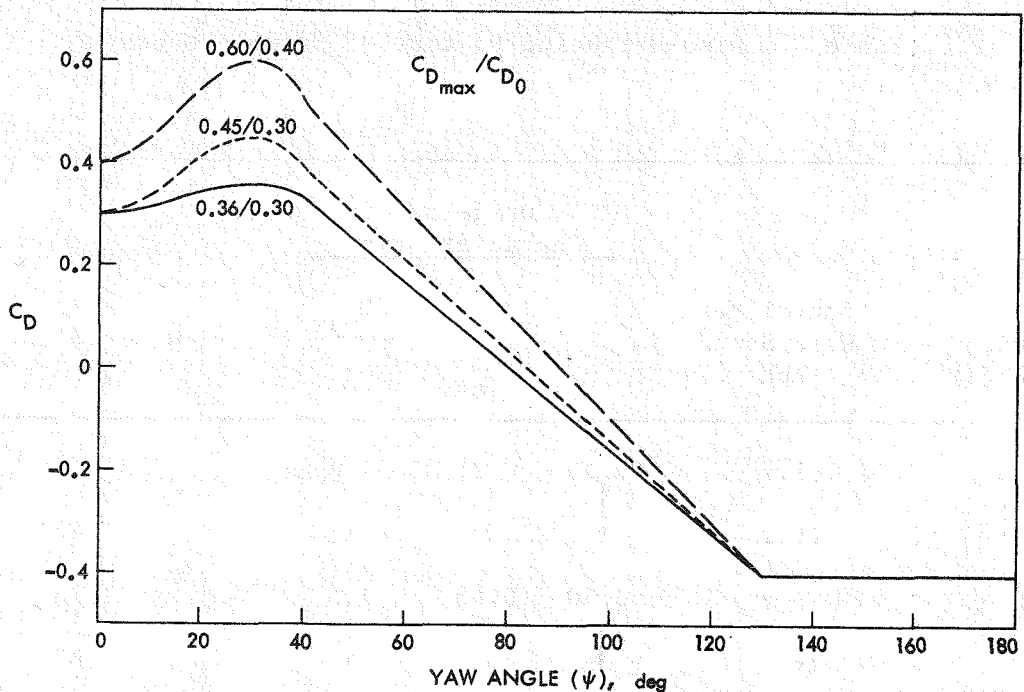


Figure 13. Aerodynamic Drag Coefficient as a Function of Yaw Angle (Parametric Variations Used in the Analysis)

simplicity, the three curves are characterized by their ratios of  $C_{D_{\max}}/C_{D_0}$  where  $C_{D_{\max}}$  occurs at  $\psi = 30$  degrees. The two upper curves show a 50% increase in  $C_D$  at  $\psi = 30$  degrees from zero-yaw levels of  $C_{D_0} = 0.4$  and 0.3; the lower curve represents a much more conservative 20% increase from  $C_{D_0} = 0.3$ \*

The wind-weighting factors resulting from variations in these parameters are shown in Table 3. Note that a zero-yaw drag coefficient must be increased by as much as 65% (wind-weighting factor = 1.65) to properly simulate a B cycle in the presence of a 16.1 kph annual mean wind speed.\*\* Similarly, the factor is only 1.2 for the D cycle; the average vehicle speed is much higher and therefore the resulting effects on yaw angle and relative wind speed are lower.

Clearly, accounting for the realistic presence of winds can significantly alter the aerodynamic input values in computer simulators. These rigorous procedures require a significant amount of computer time. A close review of the results, however, has revealed some general relationships which make simpler, closed form equations adequate in most cases. These equations and the procedure for easily incorporating this cycle-sensitive wind weighting method appears in Appendix C.

\*The vehicles listed in Section III had  $C_{D_{\max}}/C_{D_0}$  ratios from 1.2 to 1.80. The higher values were typical of high fineness ratio vehicles and windows open configurations.

\*\*This is the annual average wind speed in the U.S. measured at about 10 meters above the ground (Reference 1). Correcting for the ground boundary layer, a value of 12 kph is more suitable for automobile evaluations.

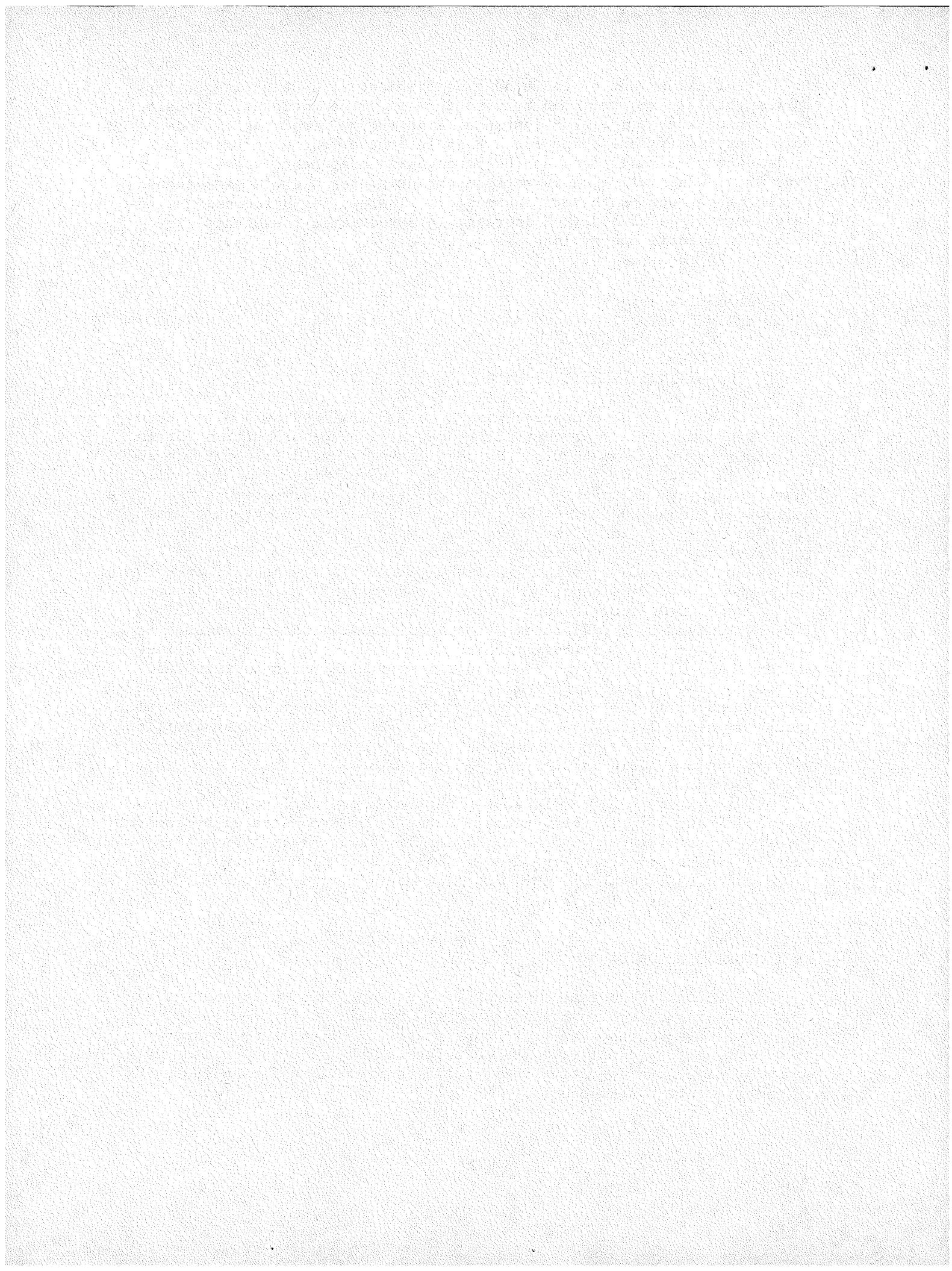
Table 3. Wind-Weighting Factors of Example Cases\*

Cycle (J227a)	Annual Mean Wind Speed kph	Drag-Yaw Characteristic			Wind-Weighting Factor
		$C_{D0}$	$C_{D\max}$	$\frac{C_{D\max}}{C_{D0}}$	
B	9.7	0.30	0.36	1.2	1.22
	16.1	↓	↓	↓	1.46
	9.7	0.30	0.45	1.5	1.33
	16.1	↓	↓	↓	1.65
	9.7	0.40	0.60	1.5	1.33
	16.1	↓	↓	↓	1.65
	9.7	0.30	0.36	1.2	1.11
	16.1	↓	↓	↓	1.25
C	9.7	0.30	0.45	1.5	1.17
	16.1	↓	↓	↓	1.37
	9.7	0.40	0.60	1.5	1.17
	16.1	↓	↓	↓	1.37
	9.7	0.30	0.36	1.2	1.05
	16.1	↓	↓	↓	1.12
	9.7	0.30	0.45	1.5	1.08
	16.1	↓	↓	↓	1.20
D	9.7	0.40	0.60	1.5	1.08
	16.1	↓	↓	↓	1.20

\*See Appendix C for generalized equations.

The final effect of these drag coefficient wind-weighting factors on the total energy consumed by a vehicle over the cycle is obviously a function of the cycle. For instance, even though aerodynamic wind-weighting factors are large for a B cycle, the effect upon the total cycle energy is small because the aerodynamic component is small.

Typically, wind weighting is more important over a D cycle even though  $F$  (the  $C_D$  correction factor) is smaller. That is, an aerodynamic wind-weighting factor of 1.2 (20% increase in aerodynamic resistance) may result in a total energy increase of up to 10%.



## SECTION VII

### GENERAL AERODYNAMIC DESIGN PRINCIPLES

The purpose of this section is to compile aerodynamic design guidelines which may be useful to EHV engineers. Though not intended to replace wind tunnel testing as a design optimization tool, these principles and procedures can provide the necessary insight to avoid certain elementary pitfalls.

Automotive aerodynamics is characterized by ground interference and large areas of separated and vortex flow. Unlike aircraft aerodynamics, it is largely unresponsive to classical analytical treatment. It has therefore become a rather empirical science, relying heavily on development through wind tunnel test techniques.

Although many of the principles involved in low-drag designs have long been known, the drag coefficient of the average production car in the early 1920s was about 0.8. By 1940 it had dropped to about 0.6 and by 1960 to about 0.5. Further improvement has come slowly, especially in this country, and the average drag coefficient of domestic automobiles has actually increased slightly in recent years with the trend toward more formal styling with less rounding of edges. Most recently, however, the pressures brought by federally mandated fuel economy requirements have sparked renewed interest in reducing aerodynamic losses. In Europe, the current average production car drag coefficient is somewhat lower, about 0.46. Drag coefficients as low as 0.15 were reported as early as 1922 by W. Klemperer (Reference 7) on an elongated teardrop automobile model. A. Morelli in 1976 (Reference 8) developed (in full-scale mock-up) a body shape encompassing a reasonable four-passenger compartment and engine cooling airflow with a drag coefficient of 0.172. Daimler-Benz recently unveiled the new experimental Mercedes C-111/3, a turbodiesel which set several speed records and is reported to have a drag coefficient of 0.195 (Reference 9). Perhaps the lowest recorded drag coefficient for a real ground vehicle is 0.12 for the Goldenrod, which holds the land speed record for wheel-driven vehicles (Reference 10). It appears, then, that there exists a rather large gap between the drag level of today's automobile and what is theoretically possible as demonstrated by some of these very specialized vehicles. Obviously, there are many practical constraints on production automobiles which compromise efforts to achieve low drag levels. However, the hope of eventually cutting present-day production car drag levels nearly in half may not be completely unrealistic.

#### A. SOURCES OF DRAG

The actual mechanisms of automotive drag production are not at all well understood. Reference 11 and others break down the sources of drag into five basic categories: (1) form drag, (2) interference drag, (3) internal flow drag, (4) surface friction drag, and (5) induced drag. A simple schematic depicting their relative importance for an IC engine car is recreated in Figure 14.

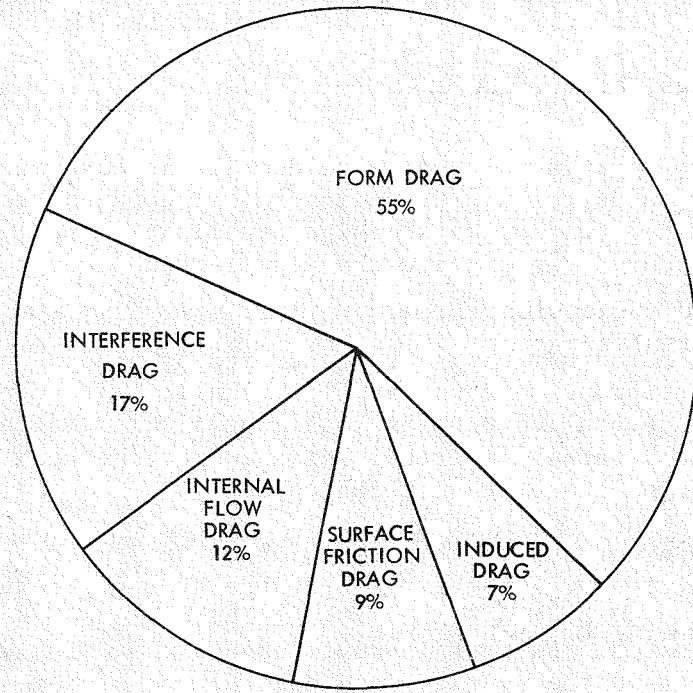


Figure 14. Distribution of IC Engine Vehicle Aerodynamic Drag (Reference 11)

Form drag (sometimes called profile drag) is a function of the basic body shape. Bodies which minimize the positive pressure on the nose and the negative pressure on the tail will exhibit lower form drag. For example, a flat plate positioned normal to the flow would represent a worst case, whereas a streamlined teardrop shape would be characteristic of minimum form drag.

Interference drag develops as the flow over the many exterior components of a vehicle body interacts with the flow over the basic shape or the flow due to the constraining influence of the ground. Various component projections such as a hood ornament, windshield wiper, radio antenna, sideview mirrors, door handles, luggage rack, rain gutters, and underbody protuberances all contribute to the interference drag component. For example, (Reference 11), a sideview mirror in a free airstream may have a drag force of 1 pound. In close proximity to the vehicle body, where the local airflow is accelerated by 25-30%, the drag on the mirror may be 1.6 pounds -- a 60% increase! Since a sideview mirror usually has a large flat aft end, it spreads a turbulent wake behind it which disturbs the basic flow on the side of the vehicle, adding a further drag increment. Projecting elements usually cause less interference on high-drag body shapes than on low-drag bodies. Since a high-drag body is usually characterized by extensive regions of separated flow, many of these elements are hidden in the already disturbed flow pattern. Conversely, the low drag of an efficient body is the result of a high degree of flow attachment. That condition is usually tenuous and any projection from the surface may cause separation. The underbody projections are some of the prime offenders as the

installation of a smooth belly pan has demonstrated many times (Reference 3). In the case of electric vehicles the traditional reasons for not using a smooth belly pan -- such as ease of maintenance, safety (oil drippings, etc.), and engine cooling restrictions -- do not apply.

Internal flow drag arises because air is required to move through the vehicle as well as around it. A conventional water-cooled IC engine requires a substantial amount of radiator airflow. Typically, the flow path is highly inefficient as local stagnation areas develop in the engine compartment and the exit path is filled with struts, hoses, brackets, and suspension elements. Here again, an electric vehicle may have an inherent advantage since its cooling requirement may be an order of magnitude less. However, ventilation of the passenger compartment is an important comfort and noise consideration, and care must be taken to design and locate the inlets and exits properly. The conventional approach is to place a flush inlet in a relatively high pressure region (usually at the base of the windshield) and either place exits in a low pressure region around the rear window or rely on normal body leaks. Unless a scoop is placed out in the flow (in which case there is an interference drag component), the drag increment due to normal ventilation requirements is negligible.

Surface friction drag results from the boundary layer which is formed as air moves along a surface. Owing to viscous friction forces, the velocity gradient normal to the surface gives rise to a shear layer. The surface finish or small imperfections, and the size of the area exposed to the flow, determine the level of this drag component. Production car finishes (surface grain size of 0.2 to 0.5 mils) are well below the critical level where additional smoothness would reduce the local friction. A smooth, continuous surface keeps skin friction low. As the flow moves rearward along a body it continually loses energy and separation is more likely to occur in critical areas. Window frames, gaps, mismatched parts, and normal skin friction all contribute to cause a rapid buildup of the boundary layer, leading to separation and more turbulence and increasing drag.

Induced drag arises from the formation of longitudinal trailing vortices generated by the pressure differential between the vehicle's underbody and roof. The energy required to generate and support this vortex field is equivalent to the energy consumed by induced drag. Often termed "lift-induced" drag or drag due to lift, there is now real doubt that any simple relationship between lift and induced drag exists (Reference 12). It can normally be minimized by careful attention to design detail on the rear portions of the vehicle, but this usually requires an experimental approach.

## B. DRAG ESTIMATION METHODS

Many aerodynamicists have attempted to make generalizations or predictions of a vehicle's drag based on various shape characteristics (References 13, 14, 15, and 16). The usual method is to assemble a large data base and develop correlations. Perhaps the best known effort is that of R.G.S. White (Reference 13) of Britain's Motor

Industry Research Association (MIRA). Wind tunnel tests of 141 different vehicles were utilized. Each vehicle was divided into six basic zones, three of which were further subdivided. Numbers were assigned to features in each zone or subzone in an attempt to rate their obstructive effects on the airflow around the vehicle.

Rating values were assigned to each of the nine categories depending upon the vehicle's shape in those zones. The predicted drag coefficient was then determined from the following equation:

$$C_D = 0.16 + 0.0095 \times \text{Drag Rating}$$

where the Drag Rating is simply the summation of the nine individual category ratings.

By way of verification, drag estimates for 20 vehicles (mainly European) were made by White using this procedure, and were then compared to measured values. The average scatter was about 7%. It should be pointed out that the drag of these vehicles was not particularly low, and that White's procedure would not necessarily reflect the subtleties inherent in drag-optimized vehicles. Another cautionary note is that measured MIRA drag values are substantially lower than similar measurements made in other wind tunnels. The real value of this effort is the relative ordering of the aerodynamic design consequences of several shape parameters.

A second, and less rigorous "drag rating" approach to drag estimates is presented in Reference 14 (Cornish). Ten regions are defined and a rating of from 1 to 3 is assigned. On this basis, the most streamlined vehicle would have a rating (R) of 30 and the worst, a rating of 10. The resulting drag coefficient is then calculated from

$$C_D = 0.62 - 0.01 R$$

This procedure is rather crude and although no direct correlation with measured data is given, its accuracy is probably far less than the 7% reported for White's method.

Both of the two previous procedures are based upon shape correlation curves which are linear with the drag rating and are limited to conventional passenger vehicle configurations. A third estimation procedure, developed for the EPA (Pershing - Reference 15), is a "drag buildup" method based on quantitative geometric characteristics applicable to a large range of generic body shapes. The total vehicle drag coefficient is defined as the sum of the coefficients of 11 discrete parts.

$$C_{D_{\text{tot}}} = \sum_{i=1}^{11} C_{D_i}$$

Only a few simple validation checks have been made, since a large data base was unavailable at the time of publication. Therefore, no accuracy claims were made. The EPA is currently sponsoring a data base development which will be used to tune and expand these procedures, make validation checks, and establish confidence levels.

Excerpts from References 13, 14, and 15 appear in Appendix D in sufficient detail to allow use of the procedures they describe.

Though not fully developed, Reference 12 (Hucho) suggests that drag may correlate well with a parameter,  $K$ , which is the line integral of the rate of change of curvature,  $k$ , of the body surface contour. For simplicity, the integral is taken for the centerline cross-section only. Applied to the entire body surface, even better correlation is expected. For a streamlined body, the rate of change of curvature along its contour is only moderate. If there are no abrupt changes in curvature, the contour parameter,  $K$ , is small. Notchback cars, on the other hand, are characterized by several steep curvature gradients, giving rise to a large value of  $K$ . It is pointed out, however, that for low drag, a small value of  $K$  is a necessary but not sufficient condition. This approach represents a much less subjective means of evaluating a vehicle body shape for drag estimates.

General rule-of-thumb values have been given to many interference components and drag reduction devices. These are helpful only in the broadest sense; that is, most effects are a function of the specific application. For instance, a front air dam (or chin spoiler) might significantly reduce the drag for one vehicle but increase it for another. Similarly, some low-drag device may be detrimental at a yaw angle. Such dramatic results, however, are generally reserved for special cases. If one limits the application to an "average, conventional sedan," perhaps the generalizations in Table 4 can provide some guidelines. The increments should not be considered as purely additive; this is particularly obvious in the case of an underpan and air dam.

The three estimating procedures and component generalizations all assume that the vehicle is traveling in a zero-wind environment. Statistically, as discussed above, a 5 to 10 mph wind is always present; the vehicle is therefore always operating at some significant angle of yaw (see Section VI). A knowledge of the specific yaw characteristics generated in the wind tunnel is necessary in order to be rigorous. However, a general equation describing the approximate shape of the  $C_D$  versus yaw angle ( $\psi$ ) has been developed by Bowman (Reference 16). Once the zero-yaw drag coefficient ( $C_{D0}$ ) has been estimated, the yaw curve may be calculated from:

$$C_D = C_{D0} + K_i (1 - \cos 6\psi)$$

Where the constant,  $K_i$ , is a function of  $C_{D0}$ ; the relationship is included as part of Appendix D (Table D-4). The yaw characteristic thus developed, the ratio  $C_{D\max}/C_{D0}$  can be determined and the effective wind-weighted drag coefficient calculated from the procedures of Section VI and Appendix C.

Table 4. Drag Increment Generalizations

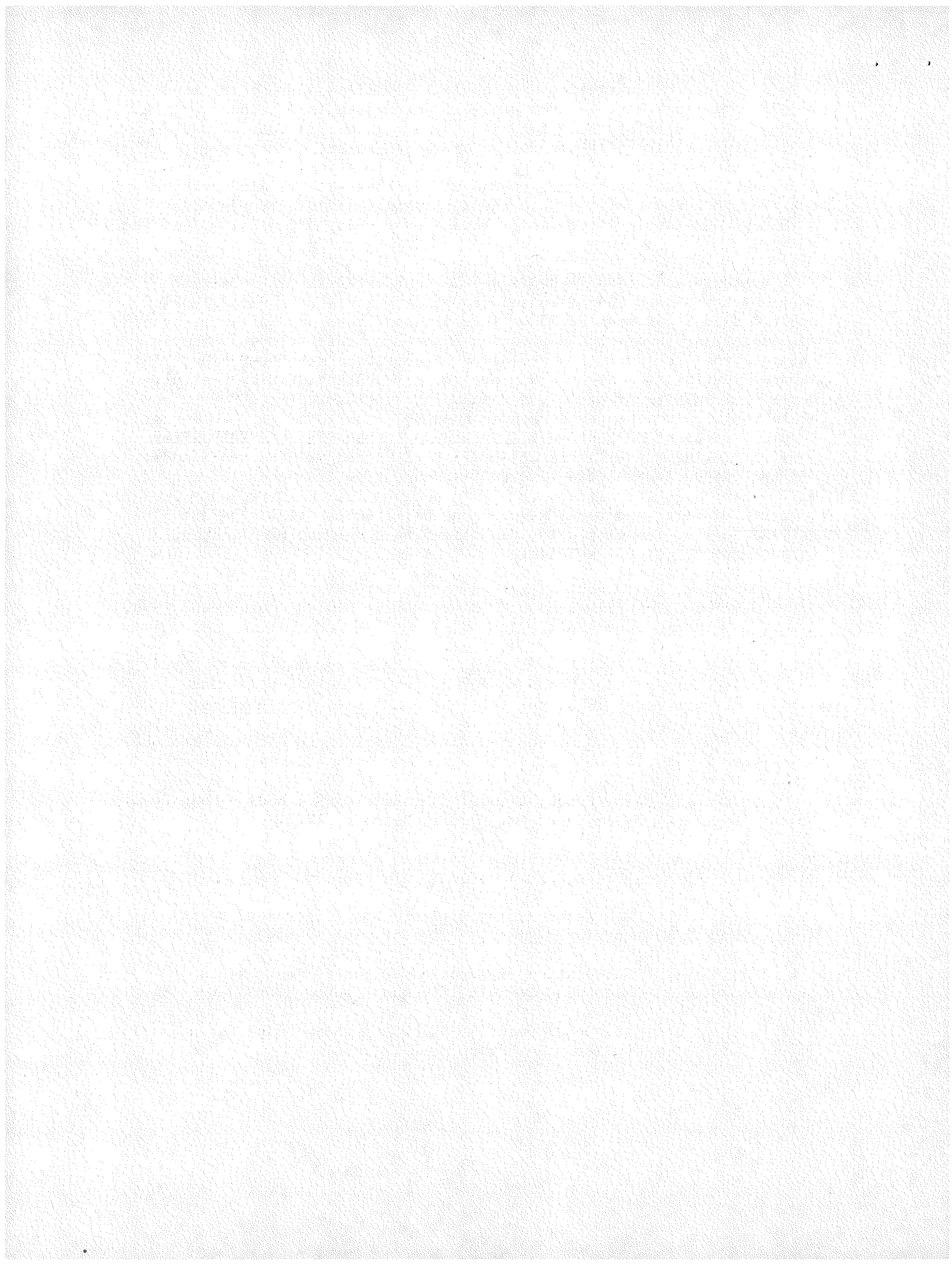
Component or Configuration	$\Delta C_D$ , (%)	Reference
Full length underpan	-5 to -15	3,17,18,19
Front "chin" spoiler (air dam)	-6 to -9	3,20,21
Rear deck spoiler (lip)	-5 to -9	3,18,20,21
Flush windshield and side glass (no raingutters)	-3 to -7	19,22
Wheel discs and rear fender skirts	-1 to -2	21
Sideview mirror	+1 to +3	11,19,22
Pop-up headlights	+3 to +6	19
Open front windows	0 to +3	3,17

Although these estimating procedures and component generalizations can provide guidance toward the development of a low-drag vehicle, it should be emphasized that design optimization can be accomplished only through development work with a wind tunnel. One can follow all the "rules" suggested by these procedures and still fall far short of the vehicle's ultimate potential. The integration and interaction of various components can present many surprises. Reference 12 points out that after separating current passenger vehicles into three classes (notchbacks, hatchbacks, and fastbacks), the centerline profiles group around an extremely narrow band; however, the corresponding drag coefficients vary by over 40%. Of course the centerline profile does not define the entire vehicle and the flow is highly three dimensional, but this suggests that drag differences are probably the result of subtle differences which cannot all be considered by estimation procedures. A case for optimizing subtle details is made in Reference 19 with respect to the General Electric Phase II Electric Vehicle which is being built under contract to the Department of Energy.\* Low drag was a major design goal and much effort was directed to that end. However, subsequent subscale wind tunnel development employing only minor cosmetic alterations to the basic design, resulted in a further 25% reduction in the drag coefficient.

\*Chrysler Corporation is the subcontractor responsible for body design.

The inherent subtleties and resulting benefits surrounding wind tunnel optimization procedures are well documented in Reference 23. A step-by-step paper approach to designing a highly efficient, low drag vehicle is not currently within the state-of-the-art. More specifically, a vehicle's aerodynamic efficiency will be a function of its design approach. For any particular design theme, there is a limit (even for experienced aerodynamicists) to the aerodynamic efficiency resulting from paper designs. Improvements beyond that point are usually a matter of chance.

Properly conducted subscale developmental testing is a valuable refinement tool and can often reduce the drag level of a "good-looking" paper design by as much as 25%. This is usually accomplished merely by cleaning up areas of flow separation exposed by tuft studies. Though a valuable tool for evaluating relative effects, the absolute values recorded during subscale testing are rarely substantiated by the full-scale vehicle. Reference 24, for example, reports  $C_{D0} = 0.30$  from subscale tests on the Copper Development Association Town Car. Full-scale results, reported in Section III, found  $C_{D0}$  to be 0.367, a 22% difference. Similarly, wind tunnel tests of a 1975 Ford Mustang II 40% scale model and the production vehicle resulted in respective drag coefficients of 0.47 and 0.53, a 12% difference. This noncorrelation is probably due to scale fidelity and local Reynolds number effects (flow separation). Full-scale wind tunnel testing can alleviate those two problems and further refine certain subtleties.



## BIBLIOGRAPHY

### A. GENERAL AERODYNAMICS

Barth, R., "Effect of Unsymmetrical Wind Incidence on Aerodynamic Forces Acting on Vehicle Models and Similar Bodies" (report abstracted from 1958 Stuttgart Thesis), A.T.Z., Mar. and Apr. 1960, pp. 89-95, MIRA Translation 15/60.

Barth, R., "Effect of Shape and Airflow about an Automobile on Drag, Lift, and Direction Control," VID, Vol. 98, No. 22, p. 1265 (in German), Aug. 1, 1956.

Bettes, W. H., "Aerodynamic Testing of High-Performance Land-Borne Vehicles-A Critical Review" in AIAA Symposium on the Aerodynamics of Sports and Competition Automobiles, Los Angeles, CA, Apr. 1968.

Bez, U., Messung des Luftwiderstandes von Kraftfahrzeugen durch Auslaufversuche, Research report, Dip. Engr. Thesis, Tech. Univer. at Stuttgart, and Porsche Research Rept., Jan. 1972.

Bowman, W. D., "The Present Status of Automobile Aerodynamics in Automobile Engineering & Development," in AIAA Symposium on the Aerodynamics of Sports and Competition Automobiles, Los Angeles, CA, Apr. 1968.

Bowman, W. D., "Generalizations on the Aerodynamic Characteristics of Sedan-Type Automobile Bodies." SAE Preprint 660389, June 6-10, 1966, SAE Transactions, June 1967.

Boyce, T. R., and Lobb, P. J. (U.K.), "An Investigation of the Aerodynamics of Current Group 6 Sport Car Designs," 'Advances in Road Vehicle Aerodynamics' 1973, pp. 127-145, BRHRA Fluid Engineering, 1973.

Buckley, B. Shaw, Laitone, Edmund V., "Airflow Beneath an Automobile," SAE Paper No. 741028, Oct. 1974.

Burst, H. E., and Srock, Lainer, "The Porsche 924 Body - Main Development Objectives," SAE Paper No. 770311, Detroit, 1977.

Carr, G. W., "The Aerodynamics of Basic Shapes for Road Vehicles, Part 2: Saloon Car Bodies," MIRA Rept. No. 1968/69.

Carr, G. W., "The Aerodynamics of Basic Shapes for Road Vehicles, Part 1: Simple Rectangular Bodies," MIRA Rept. No. 1968/2.

Carr, G. W., "Correlation of Aerodynamic Force Measurements in Quarter- and Full-Scale Wind Tunnels" (Second Report), MIRA Rept. 1967/1.

Carr, G. W., "The Development of a Low Drag Body Shape for a Small Saloon Car." MIRA Bulletin No. 2, pp. 8-14, 1965.

Carr, G. W., "Aerodynamic Effects of Modifications to a Typical Car Model," MIRA Rept. No. 1963/4.

Carr, G. W., "Aerodynamic Effects of Underbody Details on a Typical Car Model," MIRA Report 1965/7.

Carr, G. W., "Reducing Fuel Consumption by Means of Aerodynamic 'Add-on Devices'," SAE Paper No. 760187, Feb. 1976.

Choulet, R., Favero, J. L., and Romani, L., "A Study of the Aerodynamic Interaction Between a Lorry and a Car," Advances in Road Vehicle Aerodynamics 1973, pp. 255-270, BHRA Fluid Engineering, 1973.

Cornish, J. J. III, "Some Aerodynamic Characteristics of Land Vehicles," AIAA Symposium on The Aerodynamics of Sports and Competition Automobiles, Los Angeles, Apr. 1968.

Cornish, J. J., "Some Considerations of Automobile Lift and Drag," SAE Paper 948B, Jan. 11-15, 1965.

Cornish, J. J., and Fortson, C. B., "Aerodynamic Drag Characteristics of Forty-Eight Automobiles," Miss. St. Aerophysics Dept. Res. Note No. 23, June 1964.

Frackrell, J. E., and Harvey, J. K. (Imp. Col., U.K.), "The Flow Field and Pressure Distribution of an Isolation Road Wheel," 'Advances in Road Vehicle Aerodynamics' 1973, pp. 155-168, BHRA Fluid Engineering, 1973.

Flynn, H., and Kyropoulos, P., "Truck Aerodynamics," SAE Preprint 284A, 1961.

Fogg, A., and Brown, J. S., "Some Experiments on Scale-Model Vehicles with Particular Reference to Dust Entry," MIRA Report No. 1948/1.

Fosberry, R. A. C., "The Aerodynamics of Road Vehicles - A Survey of the Published Literature," MIRA Report 1958/1, p. 25.

Fugerson, W. T., "Aerodynamic Drag," Road and Track, pp. 92-98, Mar. 1966.

Goetz, H., "The Influence of Wind Tunnel Tests on Body Design, Ventilation, and Surface Deposits of Sedans and Sport Cars," SAE Paper No. 710212, Feb. 1971.

Grotewohl, A., "Seitenwinduntersuchungen an Personen-wagen ("Investigating the Effects of Cross Winds on Passenger Vehicles") Part I, A.T.Z., Vol. 69, No. 11, pp. 377-381, MIRA Translation No. 3/68, Nov. 1967.

Hawks, R. J., and Sayre (U. of Md.), "Aerodynamics and Automobile Performance," 'Advances in Road Vehicle Aerodynamics' 1973, pp. 1-13, BHRA Fluid Engineering, 1973.

Hawks, R. J., "A Tentative Model for Automobile Aerodynamics." MIT, 1966.

Hoerner, S. F., "Fluid-Dynamic Drag" Published by author (148 Busteed Dr., Midland Park, N.J.), 1965.

Howell, J. P., (City Univ., U.K.) "The Influence of the Proximity of a Large Vehicle on the Aerodynamic Characteristics of a Typical Car," 'Advances in Road Vehicle Aerodynamics' 1973, pp. 207-221, BHRA Fluid Engineering, 1973.

Hucho, W. H., Janseen, L. H., and Schwartz, G., "The Wind Tunnel's Ground Plane Boundary Layer - Its Interference with the Flow Underneath Cars," SAE Paper No. 750066, Feb. 1975.

Hucho, W. H., Jansen, L. J., and Emmelmann, H. H., "The Optimization of Body Details - A Method of Reducing the Aerodynamic Drag of Road Vehicles," SAE Paper No. 760185, Feb. 1976.

Janssch, L. H., and Hucho, W. H. (Volkswagenwerk AG, Ger. Fed. Republic), "The Effect of Various Parameters on the Aerodynamics Drag of Passenger Cars," 'Advances in Vehicle Aerodynamics' 1973, pp. 223-254, BHRA Fluid Engineering, 1973.

Janssen, L. J., and Emmelmann, H. J., "Aerodynamic Improvements - A Great Potential for Better Fuel Economy," SAE Paper No. 780265, Feb. 1978.

Kelly, K. B., and Holcombe, H. J., "Aerodynamics for Body Engineers," SAE Preprint 649A, Automobile Engineer Congress, Detroit, Jan. 14-18, 1963.

Kelly, K. B., Kyropoulos, P., and Tanner, W. F., "Automobile Aerodynamics," SAE Preprint No. 148B, SAE National Automobile Meeting, Detroit, Mar. 1969.

Kirsch, J. W., Garth, S. H., and Bettes, W., "Drag Reduction of Bluff Vehicles with Airvanes," SAE Paper No. 730686, 1973.

Klemperer, W., "Investigations of the Aerodynamics of Automobiles," Zeitschrift fuer Flugtechnik, Vol. 13, p. 201 (in German), 1922.

Koenig-Fachsenfeld, R., "Aerodynamics of Motor Vehicles," Motor Rundschau Verlag, Frankfurt A.M. (in German), 1951.

Korff, W. H., "The Body Engineer's Role in Automotive Aerodynamics," SAE Paper No. 649B, Jan. 1963.

Kosier, T. D., and McConnell, W. A., "What the Customer Gets" SAE Symposium: "Where Does All the Power Go?," SAE No. 783, June 1956.

Kuchemann, D., and Weber, J., "Aerodynamics of Propulsion," McGraw-Hill Publications in Aeronautical Science.

Kyropoulos, P., Kelly, K. B., and Tanner, W. F., "Automotive Aerodynamics," SAE Paper No. SP-180, Mar. 1960.

Lamar, P., "Aerodynamics and the Group Seven Racing Car." Presented at the AIAA Symposium on the Aerodynamics of Sports and Competition Automobiles, Los Angeles, Apr. 1968.

Larrabee, E. E., "Road Vehicle Aerodynamics or Aerodynamics as an Annoyance," Seminar paper presented at the Cranfield Institute of Technology, June 1973.

Lay, W. E., "Is 50 Miles per Gallon Possible with Correct Streamlining?", SAE Journal, Vol. 32, p. 144, 1933.

Lind, Walter, G. I., "Car Aerodynamics," Automobile Engineer, June 1958.

Lobb, P. J., The Aerodynamic Effects on Group VI Racing Cars, M.Sc. thesis, Imperial College of Science, London University, 1971.

Mair, W. A., "Reduction of Base-Drag by Boat-Tailed Afterbodies in Low-Speed Flow," Aeronautical Quarterly, Nov. 1969.

Marcell, R. P., and Romberg, G. F., "The Aerodynamic Development of the Charger Daytona for Stock Car Competition," Paper 70036, SAE Automotive Engr. Congress, Detroit, Jan. 1970.

Marte, J. E., et al., "A Study of Automobile Aerodynamic Drag," DOT-TSC-OST-75-28, Sept. 1975.

Matthews, S. A., "Aerodynamic Studies Affecting Car Performance and Appearance," Ford Motor Co. of England, Apr. 1962.

McLean, R. F., and Schilling, R., "Behind the Firebird Car's New Look," SAE Journal, Vol. 62, p. 40, Aug. 1954.

Moller, E., "Drag Measurements on the VW Delivery Truck," ATZ, Vol. 53, No. 6, p. 153, June 1951.

Morel, T., "Aerodynamic Drag of Bluff Body Shapes Characteristic of Hatch-Back Cars," SAE Paper No. 780267, Feb. 1978.

Morelli, A., "Aerodynamic Action on an Automobile Wheel," Symposium on Road Vehicle Aerodynamics, Paper No. 5, The City University, 1969.

Morelli, A., "Theoretical Method for Determining the Lift Distribution on a Vehicle," F.I.S.I.T.A., 1964.

Morelli, A., Fioravanti, L., and Cogoffi, A., "The Body Shape of Minimum Drag," SAE Paper No. 760186, Feb. 1976.

Pershing, B. (Aerospace Corp.), "The Influence of External Aerodynamics on Automotive System Design," 'Advances in Road Vehicle Aerodynamics', 1973, pp. 25-52, BHRA Fluid Engineering, 1973.

Pershing, Bernard, and Masaki, Mamoru, "Estimation of Vehicle Aerodynamic Drag," EPA-460/3-76-025, Oct. 1976.

Richie, D., "Beat the Built-In Head Wind," Commercial Car Journ., Sept. 1973.

Richie, D., "How to Beat the Built-In Head Wind," Owner-Operator, May/June, 1973.

Romani, L., "La Mesure sur Piste de la Resistance a L'avancement," Road Vehicle Aerodynamics: Proc. First Symp. Paper 15, 12 pss, City University, London, Nov. 6-7, 1969.

Romberg, G. F., Chianese, F., Jr., and Lajoie, R. G., "Aerodynamics of Race Cars in Drafting and Passing Situations," Paper 710213, SAE Automotive Engineering Congress, Detroit, Jan. 1971.

Saltzman, E. J., and Meyer, R. R., Jr., "Drag Reduction Obtained by Rounding Vertical Corners on a Box-Shaped Ground Vehicle," NASA TM X-56023, Mar. 1974.

Saltzman, E. J., Meyer, R. R., Jr., and Lux, D. P., "Drag Reductions Obtained by Modifying a Box-Shaped Ground Vehicle," NASA TM X-56027, Oct. 1974.

Schenkel, F. K., "The Origins of Drag and Lift Reductions on Automobiles with Front and Rear Spoilers," SAE Paper No. 770389, Feb. 1977.

Schlichting, H., "Aerodynamic Problems of Motor Cars," AGARD Report, 307, Oct. 1960.

Schmid, C., "Air Resistance of Automobiles," Technical University Stuttgart, VDI, Sept. 1938.

Schmid, C., "Luftwiderstand an Kraftfahrzeugen Versuche am Fahrzeug und Modell," VDI - Verlag, 1938.

Scibor-Rylski, A., (City Univ., U.K.), "Experimental Investigation of the Negative Aerodynamic Lift Wings Used on Racing Cars," 'Advances in Road Vehicle Aerodynamics' 1973, p. 147-154, BHRA Fluid Engineering, 1973.

Shapiro, A., Shape and Flow - The Fluid Dynamics of Drag, Science Study Series, Anchor Books, Doubleday and Co.

Stafford, L. G. (City Univ., U.K.), "A Numerical Method for the Calculation of Flow Around a Motor Vehicle," 'Advances in Road Vehicle Aerodynamics' 1973, p. 167-183, BHRA Fluid Engineering, 1973.

Stapleford, W. R., and Carr, G. W., "Aerodynamic Characteristics of Exposed Rotating Wheels," MIRA Report No. 1970/2.

Taylor, G. I., "Air Resistance of a Flat Plate of Very Porous Material," British Aeronaut. Research Council Rept. and Mem 2236, 1944.

Tustin, R. C., and Carr, G. W., "Aerodynamics of Basic Shapes for Small Saloon Cars," MIRA Rept No. 1965/7.

Tustin, R. C., and Carr, G. W., "Aerodynamics of Basic Shapes for Small Saloon Cars," MIRA Rept 1963/10, 23 p.

Wallis, S. B., "Ventilation System Aerodynamics - A New Design Method," SAE Paper No. 710036, Feb. 1971.

## B. FACILITY TESTING

Antonucci, G., Ceronetti, G., and Costelli, A., "Aerodynamic and Climatic Wind Tunnels in the FIAT Research Center," SAE Paper No. 770392, Feb. 1977.

Barth, R., Wind Tunnel Measurements on Vehicle Models and Rectangular Bodies with Different Proportions in Unsymmetrical Flow, Technischen Hochschule Stuttgart Thesis (in German), 1958.

Beauvais, F. N., Trignor, S. C., and Turner, T. R., "Accuracy of Car Wind Tunnel Tests Not Aided by Moving Ground Plane," SAE Journ., Vol. 77, No. 9, pp. 64-67, 1969.

Beauvais, F. N., Turner, T. R., and Tignor, S. C., "Problems of Ground Simulation in Automobile Aerodynamics," SAE Paper No. 680121, Jan. 1968.

Bettes, W. H., "Aerodynamic Testing of High Performance Land-Born Vehicles - A Critical Review," 'The Aerodynamics of Sports and Competition Automobiles - AIAA Symposium' Apr. 1968.

Bettes, W. H., and Kelly, K. B., "The Influence of Wind Tunnel Solid Boundaries on Automotive Test Data," 'Advances in Road Vehicle Aerodynamics' 1973, p. 271-290, BHRA Fluid Engineering, 1973.

Brown, G. J., and Seeman, G. R., "The Highway Aerodynamic Test Facility," AIAA Paper 72-1000, Sept. 1972, also 'Advances in Motor Vehicle Aerodynamics', 1973, pp. 323-333, BHRA Fluid Engineering, 1973.

Carr, G. W., "Aerodynamic Effects of Underbody Details in a Typical Car Model," MIRA Rept. No. 1965/7.

Carr, G. W., "The MIRA Quarter-Scale Wind Tunnel," MIRA Report No. 1961/11.

Carr, G. W., "Correlation of Pressure Measurements in Model- and Full-Scale Wind Tunnels and on the Road," SAE Paper No. 750065, Feb. 1975.

Doberenz, M. E., and Selberg, B. P., "A Parametric Investigation of the Validity of 1/25 Scale Automobile Aerodynamic Testing," SAE Paper No. 760189, Feb. 1976.

Fosberry, R.A.C., White, R.G.S., and Carr, G. W., "A British Automotive Wind Tunnel Installation and Its Application," SAE Paper 948C, Jan. 11-15, 1965.

Fosberry, R.A.C., and White, R.G.S., "A 250 hp Chassis Dynamometer," MIRA Rept. No. 1963/9.

Fosberry, R.A.C., and White, R.G.S., "The MIRA Full-Scale Wind Tunnel," MIRA Rept. No. 1961/8.

Fosberry, R.A.C., and White, R.G.S., "A Wind Tunnel for Full-Scale Motor Vehicles - Design Investigation with 1/24 Scale Model," MIRA Rept. 1960/2, 24 p.

Gross, D. S., and Sekscienski, W. S., "Some Problems Concerning Wind Tunnel Testing of Automotive Vehicles," SAE Paper 660385, 1966.

Gross, D. S., "Wind Tunnel Tests of Trailmobile Trailers," third series, Univ. of Maryland Wind Tunnel Report No. 150, Apr. 1955.

Hensel, R. W., "Rectangular-Wind Tunnel Blocking Corrections Using the Velocity-Ratio Method," TN2372, NACA, June 1951.

Kamm, W., and Schmid, C., Automobile Testing, Julius Springer, Berlin, 1938.

Kessler, J. C., and Wallis, S. B., "Aerodynamic Test Techniques," SAE Detroit Section Jr. Activity, No. 660464, Feb. 1966.

Larrabee, E. E., "Small Scale Research in Automobile Aerodynamics," SAE Preprint 660384, June 1966.

Mason, W. T. and Sovran, G. (G.M), "Ground-Plane Effects on the Aerodynamic Characteristics of Automobile Models - An Examination of Wind Tunnel Test Techniques," 'Advances in Motor Vehicle Aerodynamics' 1973, pp. 291-309, BHRA Fluid Engineering, 1973.

Mason, W. T., and Sovran, G., "Ground Plane Effects on Vehicle Testing," General Motors Research Publication GMR-1378.

Mason, W. T., Beebe, R. S., and Schenkel, F. K (Research Laboratories, GM), "An Aerodynamic Test Facility for Scale-Model Automobiles," SAE Paper 730238.

Metz, L. D., and Sensenbrenner, K. (Univ. of Ill.)(N.A.R. Corp.), "The Influence of Roughness Elements on Laminar to Turbulent Boundary Layer Transition as Applied to Scale Model Testing of Automobiles," SAE Paper 730233.

Moller, E., "Wind Tunnel Measurements on Automobiles in a Cross Wind," ATZ, Vol. 53, No. 4, p. 74 (in German), Apr. 1951.

Morelli, A. (Italy), "The New Pininfarina Wind Tunnel for Full-Scale Automobile Testing," Advances in Road Vehicle Aerodynamics, 1973.

Muto, Shinri, and Ashihara, Tomo-o, "The J.A.R.I. Full-Scale Wind Tunnel," SAE Paper No. 780336, Feb. 1978.

Oda, Norihiko, and Hoshino, Teruo, "Three Dimensional Airflow Visualization by Smoke Tunnel," SAE Paper No. 741029, Oct. 1974.

Ohtani, K., Takei, M., and Sakamoto, H., "Nissan Full-Scale Wind Tunnel - Its Application to Passenger Car Design," SAE Preprint 720100, Automotive Engineering Congress, Detroit, Jan. 10-14, 1972.

Sykes, D.M. (City Univ., U.K.), "Blockage Corrections for Large Bluff Bodies in Wind Tunnels," Advances in Motor Vehicle Aerodynamics, 1973.

Turner, T. R., "Wind Tunnel Investigations of a 3/8 Scale Automobile Model over a Moving-Belt Ground Plane," NASA Tech. Note TN D-4229, Nov. 1967.

Turner, T. R., "A Moving-Belt Ground Plane for Wind-Tunnel Ground Simulation & Results for Two Jet-Flap Configurations," NASA TN D-4228, 1967.

### C. ROAD TESTING

Fuel Economy Measurement - Road Test Procedure, SAE J1082 (SAE Recommended Practice - Apr. 1974).

Brennand, J., "Electric Vehicle Tire and Aerodynamic Friction, Road Power, and Motor-Driveline Efficiency from Track Tests," SAE Paper No. 780218, Feb. 1978.

Buckley, B. S., "Road Test Aerodynamic Instrumentation," SAE Paper No. 741030, Oct. 1974.

Yasin, T. P., "The Analytical Basis of Automobile Coastdown Testing," SAE Paper No. 780334, Feb. 1978.

"A Digital Technique for the Measurement of Total Drag Deceleration of a Vehicle," MIRA Bulletin No. 1, pp. 14-20, 1959.

Carr, G. W., and Rose, J. J., "Correlation of Full-Scale Wind Tunnel & Road Measurements of Aerodynamic Drag," MIRA Rept. No. 1964/5.

Cray, R. A., "Digital Acceleration Equipment," MIRA Bulletin No. 1, pp. 11-14, 1963.

Dayman, B., Jr., "Tire Rolling Resistance Measurements From Coast-Down Tests," SAE Paper No. 760153, Feb. 1976.

Fosberry, R.A.C., and Holubecki, Z., "The Aerodynamics of Road Vehicles - Road Measurements of Drag and Comparison with Wind Tunnel Measurements," MIRA Rept. 1958/10, 11 p.

Fosberry, R.A.C., and White, R.G.S., "The Aerodynamics of Road Vehicles - A Comparison of Cars and Their Models in Wind Tunnels," MIRA Rept. 1958/9, 37 p.

Hoerner, S. F., "Determination de la Resistance Aerodynamique des Vehicules par la Methode Roue Libre," (Determination of the Aerodynamic Resistance of Vehicles by the Coastdown Method), ZVDI 79 No. 34, pp. 1028-33, Aug. 1935.

Korst, H. H., and White, R. A., "Aerodynamic & Rolling Resistances of Vehicles as Obtained from Coast-Down Experiments," 2nd International Conf. on Vehicle Mechanics, Paris, Sept. 1971.

Larrabee, E. E., "Measuring Car Drag," Road and Track, Vol. 12, No. 6, pp. 24-28.

Lucas, G. G., and Britton, J. D., "Drag Data from Deceleration Tests and Speed Measurements During Vehicle Testing," Proc. of the 1st Road Vehicle Aerodynamics Symposium, City Univ., London, Nov. 1969.

Ordonica, M. A., "Vehicle Performance Prediction," SAE Paper 650623, May 1965, and SAE Journ., Vol. 74, No. 1, pp. 101-104, Jan. 1966.

Rousillion, G., Marzin, J., and Bourhis, J. (Peugeot), "Contribution to the Accurate Measurement of Aerodynamic Drag by the Deceleration Method," 'Advances in Road Vehicle Aerodynamics' 1973, pp. 53-66, BHRA Fluid Engineering, 1973.

Saltzman, E. J., and Meyer, R. R., Jr., "Drag Reduction Obtained by Rounding Vertical Corners on a Box-Shaped Ground Vehicle," NASA TM X-56023, Mar. 1974.

Walston, W. H., Jr., Buckley, F. T., Jr., and Marks, C. H., "Test Procedures for the Evaluation of Aerodynamic Drag on Full-Scale Vehicles in Windy Environments," SAE Paper No. 760106, Feb. 1976.

White, J. F., "New Techniques for Full-Scale Testing," SAE Preprint No. 148E, SAE National Automobile Meeting, Detroit, Mar. 1960.

White, R. A., and Korst, H. H., "The Determination of Vehicle Drag Contributions from Coast-Down Tests," SAE Paper 720099, 1972. Also, 'Advances in Road Vehicle Aerodynamics' 1973, pp. 15-23, BHRA Fluid Engineering, 1973.

Schmid, C., "Aerodynamic Drag of Motor Vehicles: Experiments with Full-Scale Car and Model," Deutsche Kraftfahrforschung, No. 1, 1938, VDI Verlag (in German).

Sherman, D., "Project Car: Crisis-Fighter Z-Car," Car and Driver, May 1974.

Sherman, D., "Project Car: Crisis-Fighter Pinto," Car and Driver, Mar. 1974.

Sturm, J. M., "Acceleration and Fuel Measurements - New Tools and Techniques," SAE Paper 471G, Jan. 1972.

#### D. NOISE

McDaniel, D. W., "Hushing Automobile Noises," SAE Preprint No. 477A, Automotive Engineering Congress, Detroit, Jan. 1972.

Richardson, E. J., "Isolation and Cure of Wind Noises," SAE Special Publication 195, pp. 14-31, Feb. 1961.

Oswald, L. J., and Dolby, D. A., "A Technique for Measuring Interior Wind Rush Noise at the Clay Model Stage of Design," SAE Paper No. 770394, Feb. 1977.

Romberg, G. F., and Lajoie, R. G., "An Objective Method of Estimating Car Interior Aerodynamic Noise," SAE Paper No. 770513, Feb. 1977.

Wattanabe, Masaru, Harita, Mituyuki, and Hayashi, Eizo, "The Effects of Body Shapes on Wind Noise," SAE Paper No. 780266, Feb. 1978.

#### E. STABILITY AND HANDLING

Basso, G. L., "Functional Derivation of Vehicle Parameters for Dynamic Studies," National Aeronautical Establishment LTR-ST. 47, Ottawa, Canada, Sept. 1974.

Hawks, R. J., The Effect of Aerodynamic Forces on the Performance and Handling Qualities of High-Speed Automobiles, Ph.D. Dissertation, Univ. of Maryland, Jan. 1972.

Hawks, R. J., and Larrabee, E. E., "The Calculated Effect of Cross Wind Gradients on the Disturbance of Automobile Vehicles," presented at AIAA Symposium on the Aerodynamics of Sports and Competition Automobiles, Los Angeles, Apr. 1968.

Korff, W. H., "The Aerodynamic Design of the Goldenrod to Increase Stability, Traction and Speed," presented at AIAA Symposium on the Aerodynamics of Sports and Competition Automobiles, Los Angeles, Apr. 1968.

Lay, W. E., and Letts, P. W., "Wind Effects on Car Stability," SAE Transactions, Vol. 61, p. 608, 1953.

Mahig, J. (Univ. of Fla.), "Variation in Vehicle Handling Characteristics Under Gusty Conditions," Advances in Road Vehicle Aerodynamics, 1973.

Moncarz, H. J., Barlow, J. B., and Hawks, R. J. (Univ. Md.), "Stability and Cross-Wind Response of an Articulated Vehicle with Roll Freedom," Advances in Road Vehicle Aerodynamics, 1973.

Weir, P. H., Heffley, R. K., and Ringland, R. F., "Simulation Investigation of Driver/Vehicle Performance in a Highway Gust Environment," 8th Annual Conference on Manual Control, May 1972.

Yoshida, Yasushi, Muto, Shinri, and Imizumi, Tetsuo, "Transient Aerodynamic Forces and Moments on Models of Vehicles Passing Through Cross-Wind," SAE Paper No. 770391, Feb. 1977.

#### F. GENERAL, BOOKS, PROCEEDINGS

Vehicle Dynamics Terminology, SAE J67d, SAE Handbook Supplement J671, published 1965.

Bekker, M. G., Theory of Land Locomotion, University of Michigan Press, Ann Arbor, 1956.

Bussien, R. (editor), Automobiltechnisches Handbuch, Technischer Verlag, Herbert Cram, Berlin, 1942.

Hayes, M. R., and Bannister, B., "Auto Union Audi Saloon Car," MIRA Rept. No. V.A. 21, 21 p., 1963.

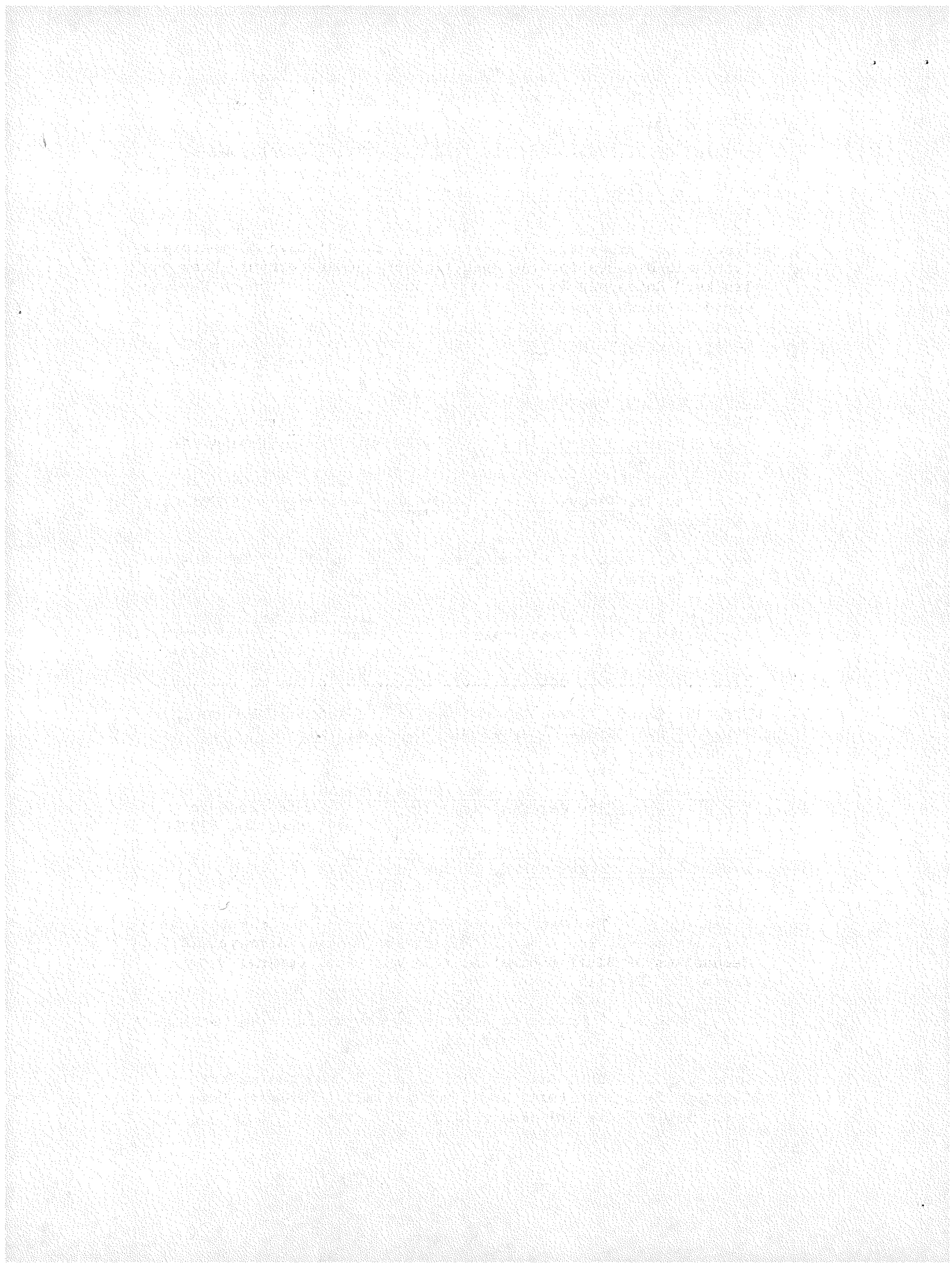
Kamm, W., Das Kraftfahrzeug (The Motor Vehicle).

Whitelaw, R. L., "Three Imperatives in the Automobile Future," Proceedings of the Second International Conf. on Vehicle Mechanics, Paris VI University, Sept. 1971.

Aerodynamics of Sports and Competition Automobiles, edited by Bernard Pershing, AIAA Symposium, May 1974.

Advances in Road Vehicle Aerodynamics, 1973, edited by H. S. Stephens, BHRA Fluid Engineering, 1973.

Automotive Aerodynamics, SAE/PT-78/16 (selected SAE Papers through 1977).



## REFERENCES

1. Buckley, F. T. Jr., and Sekscienski, W. S., "Comparisons of Effectiveness of Commercially Available Devices for the Reduction of Aerodynamic Drag on Tractor Trailers," SAE Paper No. 750704, Feb. 1975.
2. Cooper, K. R., "Wind Tunnel Investigations of Eight Commercially Available Devices for the Reduction of the Aerodynamic Drag on Trucks," Roads and Transportation Association of Canada National Conference, Quebec, Sept. 1976.
3. Marte, J. E., Weaver, R. W., Kurtz, D. W., and Dayman, B. Jr., "A Study of Automotive Aerodynamic Drag," DOT-TSC-OST-75-28, Sept. 1975.
4. Dayman, B., "Realistic Effects of Winds on the Aerodynamic Resistance of Automobiles," SAE Paper No. 780337, Feb. 1978.
5. Dayman, B., "Computer Program for Determining the Realistic Effects of Winds on the Aerodynamic Resistance of Automobiles - CARYAW," JPL Report No. 5030-175, Dec. 1977.
6. Dayman, B., "Effects of the Shape of the  $C_D$  vs  $\psi$  Curve on the Correction Factors for Realistic Effects of Winds on the Aerodynamic Resistance of Automobiles," JPL Report 5030-240, 1978.
7. Klemperer, W., "Luftwiderstandsuntersuchungen an Automobilmodellen," Zeitschrift f. Flugtechnik und Motorluftschiffahrt 13 (1922), S. 201-206.
8. Morelli, A., et al., "The Body Shape of Minimum Drag," SAE Paper No. 760186, Detroit, Feb. 1976.
9. Autoweek, May 26, 1978.
10. Korff, W. H., "The Aerodynamic Design of the Goldenrod--to Increase Stability, Traction and Speed," SAE Paper No. 660390.
11. Kelly, K. B., and Holcombe, H. J., "Aerodynamics for Body Engineers," SAE Paper No. 649A, Jan. 1963.
12. Hucho, W. H., "The Aerodynamic Drag of Cars - Current Understanding, Unresolved Problems and Future Prospects," Aerodynamic Drag Mechanisms of Bluff Bodies and Road Vehicles, General Motors Symposium, Detroit, Sept. 1976.
13. White, R.G.S., "Method of Estimating Automobile Drag Coefficients," SAE Paper No. 690189, Detroit, Jan. 1969.
14. Cornish, J. J. III, and Fortson, C. B., "Aerodynamic Drag Characteristics of Forty-eight Automobiles," Research Note No. 23, Mississippi State University, June 1964.

15. Pershing, B. and Masaki, M., "Estimation of Vehicle Aerodynamic Drag," EPA-460/3-76-025 Aerospace Corporation, El Segundo, 1976.
16. Bowman, William D., "Generalizations on the Aerodynamic Characteristics of Sedan Type Automobile Bodies," SAE Paper No. 660389, Detroit, Jan. 1966.
17. Fluid-Dynamic Drag, Sighard F. Hoerner, published by the author, 1958.
18. Ohtani, K., et al., "Nissan Full-Scale Wind Tunnel--Its Application to Passenger Car Design," SAE Paper No. 720100, Detroit, 1972.
19. Near Term Electric Vehicle, Phase II Mid-Term Summary Report, Contract No. EY-76-C-03-1294, General Electric Co., Schenectady, N.Y., July 1978.
20. Schenkel, F. K., "The Origins of Drag and Lift Reductions on Automobiles with Front and Rear Spoilers," SAE Paper No. 770389, Detroit, 1977.
21. Carr, G. W., "Reducing Fuel Consumption by Means of Aerodynamic "Add-on" Devices," SAE Paper No. 760187, Detroit, 1976.
22. Korff, W. H., "The Body Engineer's Role in Automotive Aerodynamics," Paper No. 649 B, Automotive Engineering Congress, Jan. 1963.
23. Hucho, W. H., Janssen, L. J., and Emmelmann, H. J., "The Optimization of Body Details - A Method for Reducing the Aerodynamic Drag of Road Vehicles," SAE Paper No. 760185, Feb. 1976.
24. Pocabello, M., and Armstrong, D., "The Copper Electric Town Car," SAE Paper No. 760071, Feb. 1976.

APPENDIX A

EHV SOURCE LIST

A Request for Quotation was sent to the following possible owners or developers of electric or hybrid vehicles asking for the use of a vehicle for aerodynamic characterization testing.

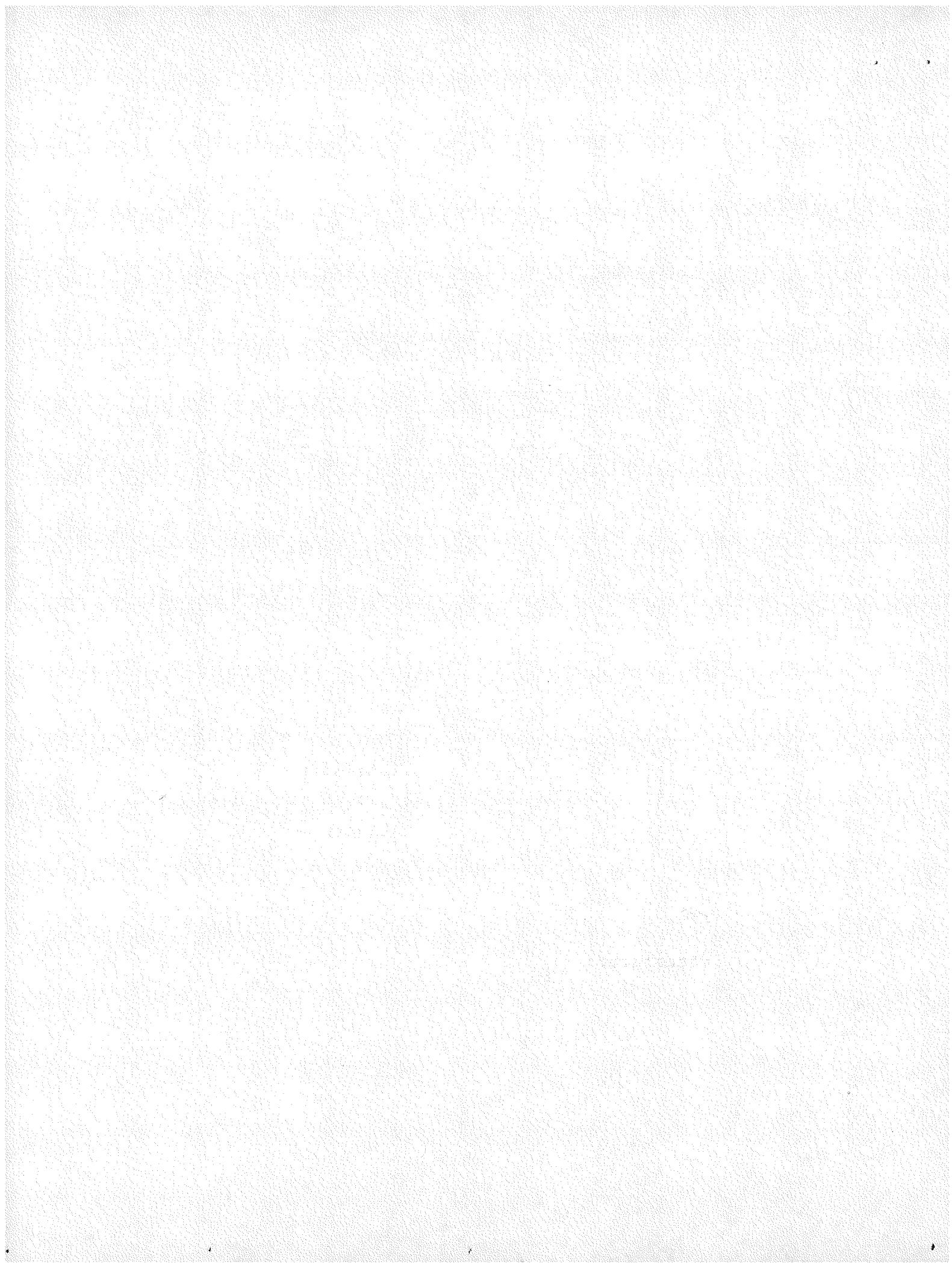
1. AIL Division of Cutler-Hammer  
Transportation System Division  
Farmingdale, NY 11735
2. Anderson Power Products  
145 Newton Street  
Brighton, MA 02135
3. Copper Development Association  
Attn: Mr. Don Miner, Manager  
430 N. Woodward Avenue  
Birmingham, MI 48011
4. Elcar Corporation  
Attn: Leon Shalmasarian, Pres.  
2118 Bypass Road  
P. O. Box 937  
Elkhart, IN 46514
5. Elec-Traction  
Heybridge Basin,  
Maldon, Essex  
England
6. Electra-Van  
A Division of Jet Industries  
Attn: William Bales, Pres.  
2503 Edgewater Drive  
Austin, TX 78746
7. Electric Vehicle Engineering  
Attn: Wayne Goldman, Pres.  
P. O. Box 1  
Lexington, MA 02173
8. Energy Research & Development  
Corp.  
Attn: Robert Childs, Pres.  
9135 Fernwood Drive  
Olmsted Falls, Ohio 44138
9. ESB, Inc.  
Attn: Jim Norberg  
P. O. Box 8109  
Philadelphia, PA 19109
10. Exxon Enterprises  
Electric Power Conversion  
Systems Project  
Attn: R. L. Ricci  
P. O. Box 192  
Florham Park, NY 07932
11. Fiat  
Attn: G. Brusaglino  
10 Corso Marconi  
Turin, Italy
12. General Electric Co.  
Corporate Research & Development  
Attn: Robert Guess  
Bldg. 37 Rm. 2083  
One River Road  
Schenectady, NY 12301
13. General Motors Technical Center  
General Motors Transportation  
Systems Division  
Attn: S. Romano, Mgr.,  
Systems Applications  
Warren, MI 48090
14. Globe Union, Inc.  
Globe Battery Division  
Attn: Mr. Vicent Hasall  
5757 North Green Bay Avenue  
Milwaukee, WI 53201
15. Kaylor Energy Products  
Attn: Roy Kaylor, Pres.  
1918 Minelto Avenue  
Menlo Park, CA 94025

16. Dr. H. D. Kesling  
TP Laboratories  
P. O. Box 73  
La Porte, IN 46350
17. Lucas Industries Limited  
Great King Street  
Birmingham, B192 XF  
England
18. Marathon Electric Vehicles  
A Div. of Marathon Golf Car Ltd.  
8305 Le Creusot Street  
Montreal, Quebec HIP 2A2
19. McKee Engineering Corporation  
Attn: Robert McKee, Pres.  
411 West Colfax  
Palatine, IL 60067  
(312) 358-6773
20. Minicars, Inc.  
Attn: Donald Wahl  
35 La Patera Lane  
Goleta, CA 93017
21. Wally E. Rippel  
700 W. Sierra Madre Blvd., Apt. 29  
Sierra Madre, CA 91024
22. Paul R. Shipps  
3 E. Vehicles  
P. O. Box 19409  
San Diego, CA 92119
23. Structural Plastics, Inc.  
Attn: William Gillespie, Pres.  
1133 S. 120th East Avenue  
Tulsa, OK 74128
24. Titan, Inc.  
P. O. Box 912  
Temple City, CA 91780
25. University of British Columbia  
Depart. of Mechanical Engineering  
Attn: Dobzosav Ratajac  
Vancouver, B.C.

## APPENDIX B

### WIND-WEIGHTING PROGRAM (EHVSCD):

- (1) SOURCE LISTING, (2) EXAMPLE RESULTS



## PROGRAM LISTING

\* \* \* \* \* UNITVAC 1100 TIME-SHARING EXEC --- MULTI-PROCESSOR SYSTEM --- VER. 051178-FV338 SITE \* 1108C \* \* \* \* \*

RUNID \* EHVSCD BLDG/BOX \* B4TN 198634 PART NUMBER \* 00 INPUT DEVICE \* G9CRDK OUTPUT DEVICE \* G9HSRK

FILE NAME \* PR0000EHVS00 CREATED AT 03121839 MAY 13, 1978 PRINTED AT 03139136 MAY 13, 1978

## PROGRAM LISTING

## PROGRAM LISTING

## PROGRAM LISTING

```

00262 107* PWRMXB=0.0
00263 108* DO 100 IS1,47
00266 109* IF(I.GT.19) DVDT(I)=0.0      * PERFORM COMPUTATION FOR SAE B CYCLE
00270 110* IF(I.GT.38) DVDT(I)=32.14*(AEROF+RRF)/(W*BETA*F)  * CONSTANT SPEED DURING CRUISE
00272 111* IF(I.GT.42) DVDT(I)=BRKDEC  * DECEL DURING COAST
00274 112* V=V+DVDT(I)              * INTEGRATE DV/DT TO GET VEHICLE SPEED
00275 113* IF(J.EQ.42) BRKDEC=V/5.0  * DECELERATION NECESSARY TO STOP
00277 114* IF(VEL.GT.V) VEL=V      * IDENTIFY MINIMUM VELOCITY (END OF CYCLE)
00301 115* IF(V.LT.0.0) V=0.0      * ELIMINATE POSSIBILITY OF ROUNDOFF ERROR
00303 116* P=V*F/550.             * CONVERSION FACTOR TO HP
00304 117* X=WIND(J)*SIN(PHI/IRD) * CALCULATE CROSS-WIND COMPONENT
00305 118* Y=WIND(J)*COS(PHI/IRD) * CALCULATE PARALLEL WIND COMPONENT
00306 119* VR=SQRT(X**2+(Y**2))  * CALCULATE RELATIVE WIND TO VEHICLE
00307 120* YAW=RD*ATAN(X/(Y+V+0.0001)) * CALCULATE INSTANTANEOUS WIND YAW ANGLE
00310 121* IF(YAW.LT.0.0) YAW=180.0+YAW  * NEG YAW INDICATES POS TAIL-WIND DIRECTI
00312 122* VPLUSY=V+Y
00313 123* IF(PHI.EQ.180.0.AND.VPLUSY.LT.0.0) YAW=180.0
00315 124* IF(IMISC3.EQ.3012) CD=0.30+0.0002*YAW**2=0.0000044444*YAW**3 3012=1
00317 125* IF(IMISC3.EQ.3012.AND.YAW.GT.40.0) CD=0.3356+0.7356*(YAW=40.0)/90. 3012=2
00321 126* IF(IMISC3.EQ.3015) CD=0.30+0.0005*YAW**2=0.00001111*YAW**3 3015=1
00323 127* IF(IMISC3.EQ.3015.AND.YAW.GT.40.0) CD=0.389+0.789*(YAW=40.0)/90.0 3015=2
00325 128* IF(IMISC3.EQ.4015) CD=0.40+0.001333*YAW**2=0.0000296*YAW**3 4015=1
00327 129* IF(IMISC3.EQ.4015.AND.YAW.GT.40.0) CD=0.60+1.14*(YAW=40.0)/90.0 4015=2
00331 130* IF(YAW.GT.130.0) CD=0.40  ALL
00333 131* CDZERO=FLOAT(IMISC3/100)/100.0  * ZERO-YAW CD
00334 132* IF(J.EQ.14) CD=CDZERO*(0.6+0.05*FLOAT(K-1))  * FOR VARIOUS CONSTANT CD'S
00336 133* IF(J.EQ.14) VR=V  * FOR CD/CD0 VARIATION USE VEHICLE SPEED
00340 134* AEROF=0.5*H0*F*CD*VR**2*F**2  * AERODYNAMIC DRAG FORCE
00341 135* RRF=(W-ELTOD*ABS(AEROF))*(C0+C1*V+C2*V**2+C3*V**3)  * ROLL RESIST FORCE
00342 136* BETA=1.4  * LOW GEAR ENGINE ROTATIONAL INERTIA
00343 137* IF(V.GT.10.0) BETA=1.2  * SECOND GEAR ENGINE ROTATIONAL INERTIA
00345 138* IF(V.GT.20.0) BETA=1.1  * HIGH GEAR ENGINE ROTATIONAL INERTIA
00347 139* IF(DVDT(I).LT.0.1) BETA=1.035  * NO ENGINE ROT INERTIA FOR COASTING
00351 140* IF(IMISC4.EQ.1) BETA=1.035  * ASSUME CONSTANT INERTIA MASS
00353 141* DVDTF=W*BETA*DVT(I)*F/32.16  * ACCELERATION FORCE
00354 142* ROOT=1.0/FLOAT(IMISC2)  * ROOT FOR MOTOR EFFICIENCY FACTOR
00355 143* WFVEL=1.0/(0.1+0.9*(V/60.0)**ROOT)  * MOTOR EFFICIENCY FACTOR
00356 144* IF(IMISC1.EQ.1) WFVEL=1.0  * SET ENGINE MAP WT. FACTOR TO UNITY
00360 145* AFROHP=AEROF*PWFVEL  * HP TO OVERCOME AERO DRAG
00361 146* RRHP=RRF*PWFVEL  * HP TO OVERCOME ROLL RES
00362 147* ACCHP=(TH0K*V*V+THREEK)*(W/4000.0)*WFVEL  * HP TO OPERATE ACCESSORIES
00363 148* DVDTHP=DVDTF*PWFVEL  * HP TO ACCELERATE VEHICLE
00364 149* ARD=AEROHP+RRHP+DVDTHP  * SUMMATION OF ROAD LOADS EXCEPT ACCESSOR
00365 150* REGEN=0.01*FLOAT(IMISC5)  * REGENERATIVE BRAKING FACTOR
00366 151* IF(ARD.GE.0.0) TOTHP=1.1*ARD+ACCHP  * TOTAL HP REQD=0.9 XMS EFF
00370 152* IF(ARD.LT.0.0) TOTHP=REGEN*ARD/WFVEL+ACCHP  * REGENERATION OF POWER
00372 153* HPSEC=HPSEC+TOTHP*0.0002071  * TOTAL KWH ENERGY REQUIRED
00373 154* IF(DVDT(I).GE.0.0) TAROHP=1.1*AEROHP  * TOTAL AERO POWER REGT
00375 155* AHSEC=AHSEC+TAROHP*0.0002071  * SUM UP AERO ENERGY IN KWH
00376 156* IF(VMAXB.LT.V) VMAXB=V  * DETERMINE MAXIMUM VELOCITY
00400 157* IF(VMAXB.EQ.V) TVMAXB=FLOAT(I)  * DETERMINE TIME AT MAXIMUM VELOCITY
00402 158* S=S+(V-0.5*DVDT(I))/F/5280.0  * DISTANCE VEHICLE TRAVELS
00403 159* IF(WIND(J).LT.0.9) GO TO 199  * CALC ONLY FOR ZERO WIND CASE
00405 160* GO TO 299  * DO NOT CALC IF WIND NOT ZERO
00406 161* 199 PI=3.1415926  * CALC FOLLOWING WHEN WIND IS ZERO
00407 162* IF(I.EQ.40) DVDT40=DVDT(I)  * AVERAGE DECEL DURING COASTING
00411 163* IF(I.EQ.44) DVDT44=DVDT(I)  * DECELERATION DURING BRAKING TO STOP

```

## PROGRAM LISTING

```

00413 164* IF(I.EQ.1) APRB1= 0.746*TAROHP 0 POWER TO OVERCOME AERO RES AT 1 SEC
00415 165* IF(I.EQ.4) APRB4= 0.746*TAROHP 0 POWER TO OVERCOME AERO RES AT 4 SEC
00417 166* IF(I.EQ.9) APRB9= 0.746*TAROHP 0 POWER TO OVERCOME AERO RES AT 9 SEC
00421 167* IF(I.EQ.14) APRB14= 0.746*TAROHP 0 POWER TO OVERCOME AERO RES AT 14 SEC
00423 168* IF(I.EQ.19) APRB19= 0.746*TAROHP 0 POWER TO OVERCOME AERO RES AT 19 SEC
00425 169* IF(I.EQ.21) APRB21= 0.746*TAROHP 0 POWER TO OVERCOME AERO RES AT 21 SEC
00427 170* IF(I.EQ.1) PWRB1= 0.746*TOTHP 0 TOTAL KW AT TIMES 1 SEC FOR CYCLE B
00431 171* IF(I.EQ.4) PWRB4= 0.746*TOTHP 0 TOTAL KW AT TIMES 4 SEC FOR CYCLE B
00433 172* IF(I.EQ.9) PWRB9= 0.746*TOTHP 0 TOTAL KW AT TIMES 9 SEC FOR CYCLE B
00435 173* IF(I.EQ.14) PWRB14= 0.746*TOTHP 0 TOTAL KW AT TIME=14 SEC FOR CYCLE B
00437 174* IF(I.EQ.19) PWRB19= 0.746*TOTHP 0 TOTAL KW AT TIME=19 SEC FOR CYCLE B
00441 175* IF(I.EQ.21) PWRB21= 0.746*TOTHP 0 TOTAL KW AT TIME=21 SEC FOR CYCLE B
00443 176* TOTHPK=TOTHP*0.746 0 CONVERT HP TO KW
00444 177* IF(PWRMXB.LT.TOTHPK) PWRMXB=TOTHPK 0 DETERMINE MAX POWER USED
00446 178* IF(PWRMXB.EQ.TOTHPK) TPMAXB=FLOAT(I) 0 DETERMINE TIME AT MAX PWR
00450 179* 299 PI=3.1415926
00451 180* 100 CONTINUE
00453 181* VENDR=VEL
00454 182* DISTB=S
00455 183* AEROU(J,K)=AHPSEC/S
00456 184* TOTLU(J,K)=HPSEC/S
00457 185* S=0.0
00460 186* V=0.0
00461 187* VEL=5.0
00462 188* VMAXD=0.0
00463 189* HPSEC=0.0
00464 190* AHPSEC=0.0
00465 191* PWRMXD=0.0
00466 192* DO 101 M=1,97
00471 193* IF(M.GT.28) DVdz(M)=0.0
00473 194* IF(M.GT.7A) DVdz(M)=32.14*(AEROF+RRF)*(W*beta*f) 0 DECCEL DURING COAST
00475 195* IF(M.GE.88) DVdz(M)=BRKDEC
00477 196* V=V+DVdz(M)
00500 197* IF(M.EQ.88) BRKDEC=V/9.0
00502 198* IF(VEL.GT.V) VEL=V
00504 199* IF(VEL.LT.0.0) V=0.0
00506 200* P=V*f/550.
00507 201* X=WINDE(J)*SIN(PHI/RD)
00510 202* Y=WINDE(J)*COS(PHI/RD)
00511 203* VR=SQRT(X**2+(V+Y)**2)
00512 204* YAW=RD*ATAN2(X/(V+Y+0.0001))
00513 205* IF(YAW.LT.0.0) YAW=180.0+YAW
00515 206* VPLUSY=V+Y
00516 207* IF(PHT.EQ.180.0.AND.VPLUSY.LT.0.0) YAW=180.0
00520 208* IF(IMISC3.EQ.3012) CD=0.30+0.0002*YAW**2+0.00004444*YAW**3 3012=1
00522 209* IF(IMISC3.EQ.3012.AND.YAW.GT.40.0) CD=0.3356-0.7356*(YAW-40.0)/90. 3012=2
00524 210* IF(IMISC3.EQ.3015) CD=0.30+0.0005*YAW**2+0.0001111*YAW**3 3015=1
00526 211* IF(IMISC3.EQ.3015.AND.YAW.GT.40.0) CD=0.389-0.789*(YAW-40.0)/90.0 3015=2
00530 212* IF(IMISC3.EQ.4015) CD=0.40+0.001333*YAW**2+0.0000296*YAW**3 4015=1
00532 213* IF(IMISC3.EQ.4015.AND.YAW.GT.40.0) CD=0.64-1.14*(YAW-40.0)/90.0 4015=2
00534 214* IF(YAW.GT.130.0) CD=-0.40
00536 215* CDZERO=FLOAT(IMISC3/100)/100.0 0 ZERO=YAW CD
00537 216* IF(J.EQ.14) CD=CDZERO*(0.6+0.05*FLOAT(K-1)) 0 FOR VARIOUS CONSTANT CD'S
00541 217* IF(J.EQ.14) VREB 0 FOR CD/CD0 VARIATION USE VEHICLE SPEED
00543 218* AEROF=0.5*RHO*A*CD*VR**2*F**2 0 AERODYNAMIC DRAG FORCE
00544 219* RRF=(W*ELTOD*ABS(AEROF))*(C0+C1*V+C2*V*V+C3*V**3) 0 ROLL RESIST FORCE
00545 220* BETA=1.4 0 LOW GEAR ENGINE ROTATIONAL INERTIA

```

## PROGRAM LISTING

```

00546 221* IF(V.GT.10.0) BETA =1.2      * SECOND GEAR ENGINE ROTATIONAL INERTIA
00550 222* IF(V.GT.20.0) BETA =1.1      * HIGH GEAR ENGINE ROTATIONAL INERTIA
00552 223* IF(DVDZ(M).LT.0.1) BETA=1.035 * NO ENGINE ROT INERTIA FOR COASTING
00554 224* IF(IMISC4.EQ.1) BETA=1.035   * ASSUME CONSTANT INERTIA MASS
00556 225* ROOT=1.0/FLOAT(IMSC2)      * ROOT FOR MOTOR EFFICIENCY FACTOR
00557 226* WFVEL=1.0/(1.0+0.9*(V/60.0)**ROOT) * MOTOR EFFICIENCY FACTOR
00560 227* DVDTFBW*BETA*DVDZ(M)*F/32.16 * ACCELERATION FORCE
00561 228* IF(IMISC1.EQ.1) WFVEL=1.0   * SET ENGINE MAP WT FACTOR TO UNITY
00563 229* AEROHPSAERDF*P*WFVEL      * HP TO OVERCOME AERO DRAG
00564 230* RRHP=RRF*P*WFVEL        * HP TO OVERCOME ROLL RES
00565 231* ACCHP=(TWOKEV*V+THREEK)*(W/4000.0)*WFVEL * HP TO OPERATE ACCESSORIES
00566 232* DVDTHP=DVDTF*P*WFVEL    * HP TO ACCELERATE VEHICLE
00567 233* REGEN=0.01*FLOAT(IMSC5)  * REGENERATIVE BRAKING FACTOR
00568 234* ARD=AEROHP+RRHP+DVDTHP * SUMMATION OF ROAD LOADS EXCEPT ACCESSOR
00570 235* IF(ARD.GE.0.0) TOTHP=1.1*ARD+ACCMP  * TOTAL HP REQD=0.9 XMS EFF
00571 235* IF(ARD.LT.0.0) TOTHP=1.1*ARD+ACCMP  * TOTAL HP REQD=0.9 XMS EFF
00573 236* IF(ARD.EQ.0.0) TOTHP=1.1*ARD+ACCMP  * TOTAL KWH ENERGY REQUIRED
00575 237* HPSFC=HPSEC+TOTHP*0.0002071  * TOTAL KWH ENERGY REQUIRED
00576 238* IF(DVDZ(M).GE.0.0) TAROHP=1.1*AEROHP * TOTAL AERO POWER REQD
00600 239* AHPSEC=AMPSFC+TAROHP*0.0002071  * SUM UP AERO ENERGY IN KWH
00601 240* S=S+(V-0.5*DVDZ(M))*F/5280.0  * DISTANCE VEHICLE TRAVELS
00602 241* IF(VMAXD.LT.V) VMAXD=V  * DETERMINE MAXIMUM VELOCITY
00604 242* IF(VMAXD.EQ.V) TVMAXD=FLOAT(M)  * DETERMINE TIME AT MAXIMUM VELOCITY
00606 243* IF(WIND(J).LT.0.9) GO TO 399  * CALC ONLY FOR ZERO WIND CASE
00610 244* GO TO 499
00611 245* 399 PI=3.1415926  * DO NOT CALC IF WIND NOT ZERO
00612 246* IF(M.EQ.83) DVDT83=DVDZ(M)  * CALC FOLLOWING WHEN WIND IS ZERO
00614 247* IF(M.EQ.92) DVDT92=DVDZ(M)  * AVERAGE DECEL DURING COASTING
00616 248* IF(M.EQ.1) APRD1=0.746*TAROHP  * DECELERATION DURING BRAKING TO STOP
00620 249* IF(M.EQ.7) APRD7=0.746*TAROHP  * POWER TO OVERCOME AERO RES AT 1 SEC
00622 250* IF(M.EQ.14) APRD14=0.746*TAROHP  * POWER TO OVERCOME AERO RES AT 7 SEC
00624 251* IF(M.EQ.21) APRD21=0.746*TAROHP  * POWER TO OVERCOME AERO RES AT 14 SEC
00626 252* IF(M.EQ.28) APRD28=0.746*TAROHP  * POWER TO OVERCOME AERO RES AT 21 SEC
00630 253* IF(M.EQ.32) APRD32=0.746*TAROHP  * POWER TO OVERCOME AERO RES AT 28 SEC
00632 254* IF(M.EQ.1) PWRD1=0.746*TOTHP  * TOTAL KW AT TIME= 1 SEC FOR CYCLE D
00634 255* IF(M.EQ.7) PWRD7=0.746*TOTHP  * TOTAL KW AT TIME= 7 SEC FOR CYCLE D
00636 256* IF(M.EQ.14) PWRD14=0.746*TOTHP  * TOTAL KW AT TIME=14 SEC FOR CYCLE D
00640 257* IF(M.EQ.21) PWRD21=0.746*TOTHP  * TOTAL KW AT TIME=21 SEC FOR CYCLE D
00642 258* IF(M.EQ.28) PWRD28=0.746*TOTHP  * TOTAL KW AT TIME=28 SEC FOR CYCLE D
00644 259* IF(M.EQ.32) PWRD32=0.746*TOTHP  * TOTAL KW AT TIME=32 SEC FOR CYCLE D
00646 260* TOTHPK=TOTHP*0.746  * CONVERT HP TO KW
00647 261* IF(PWRMXD.LT.TOTHPK) PWRMXD=TOTHPK  * DETERMINE MAX POWER USED
00651 262* IF(PWRMXD.EQ.TOTHPK) TMAXD=FLOAT(M)  * DETERMINE TIME AT MAX_PWR
00653 263* 499 PI=3.1415926
00654 264* 101 CONTINUE
00656 265* VENDD=VEL  * VELOCITY AT END OF CYCLE (ZERO)
00657 266* DISTD=S  * DISTANCE TRAVELED DURING SAE D CYCLE
00660 267* AEROU(J,K)=AHPSEC/S  * CALCULATE AVG KWH PER MILE FOR AERO RES
00661 268* TOTLU(J,K)=HPSEC/S  * CALCULATE AVG TOTAL KWH PER MILE
00662 269* IF(J.NE.1) GO TO 444
00664 270* DO 333 KK=1,19  * COMPUTE ZERO-WIND SPEED ITEMS ONLY ONCE
00667 271* AEROU(J+KK)=AEROU(1,1)
00670 272* TOTLU(J+KK)=TOTLU(1,1)
00671 273* AEROH(J,KK)=AEROH(1,1)
00672 274* TOTLH(J+KK)=TOTLH(1,1)
00673 275* 333 CONTINUE
00675 276* GO TO 300
00676 277* 444 PI=3.1415926  * DUMMY STATEMENT TO GIVE A 'GO TO' ADDRESS

```

## PROGRAM LISTING

```

00677 278* 200  CONTINUE
00701 279* 300  CONTINUE
00703 280*  DO 303 J=1,13
00706 281*    AEROUA(J)=0.0
00707 282*    TOTLUA(J)=0.0
00710 283*    AEROH(A(J)=0.0
00711 284*    TOTLHA(J)=0.0
00712 285*    DO 555 K=1,19
00715 286*      STORE1=AEROU(J,K)
00716 287*      STORE2=TOTLU(J,K)
00717 288*      IF(K,EG,1,0R,K,EG,19) AEROU(J,K)=0.5*AEROU(J,K)
00721 289*      IF(K,EG,1,0R,K,EG,19) TOTLU(J,K)=0.5*TOTLU(J,K)
00723 290*      AEROUA(J)=AEROUA(J)+AEROU(J,K)/18.0
00724 291*      TOTLUA(J)=TOTLUA(J)+TOTLU(J,K)/18.0
00725 292*      AEROU(J,K)=STORE1
00726 293*      TOTLU(J,K)=STORE2
00727 294*      STORE3=AEROH(J,K)
00730 295*      STORE4=TOTLH(J,K)
00731 296*      IF(K,EG,1,0R,K,EG,19) AEROH(J,K)=0.5*AEROH(J,K)
00733 297*      IF(K,EG,1,0R,K,EG,19) TOTLH(J,K)=0.5*TOTLH(J,K)
00735 298*      AEROH(A(J)=AEROH(A(J)+AEROH(J,K)/18.0
00736 299*      TOTLHA(J)=TOTLHA(J)+TOTLH(J,K)/18.0
00737 300*      AEROH(J,K)=STORE3
00740 301*      TOTLH(J,K)=STORE4
00741 302* 555  CONTINUE
00743 303* 303  CONTINUE
00745 304*  WRITE(6,220)
00747 305* 220  FORMAT(10I,30X,'PERTINENT ZERO-WIND DRIVING CYCLE QUANTITIES//')
00750 306*  WRITE(6,230) VMAXB,TVMAXB,VENDB,DISTB,DVDT40,DVDT44,
00750 307* 1 APRB1,APRB4,APRB9,APRB14,APRB19,APRR21,
00750 308* 2 PWR1,PWR4,PWR89,PWR8914,PWR819,PWR821,PWRMXB,TPMAXB
00776 309* 230  FORMAT(10I,40X,'SAE DRIVING CYCLE B1//'
00776 310* 1 10I,15X,'VMAX=1,F6,3,IMPH(AT TIME1,F6,1,1SEC)!',
00776 311* * 5X,'VELEND=1,F6,3,IMPH1,5X,'DIST',
00776 312* 2 'TRAVELED=1,F6,3,IMILES1,1,24X,'COAST DECEL=1,F6,3,IMPHPS',
00776 313* 3 5X,'BRAKE DECEL=1,F6,3,IMPHPS1'
00776 314* 4 10I,15X,'POWER FROM BATTERY TO OVERCOME AERO RESISTANCE AT TIME1,
00776 315* 5 1,1,4,9,14,19,21 SEC1/1,25X,6F8,3,1KWH1
00776 316* 6 10I,15X,'TOTAL POWER FROM BATTERY AT TIME 1,4,9,14,19,21 SEC1,
00776 317* 7 1 AND MAX1,1,25X,6F8,3,1 KW 1,F8,3,1 (AT TIME1,F6,1,1SEC)1//'
00777 318*  WRITE(6,240) VMAXD,TVMAXD,VENDD,DISTD,DVDT83,DVDT92,
00777 319* 1 APRD1,APRD7,APRD14,APRD21,APRD28,APRD32,
00777 320* 2 PWRD1,PWRD7,PWRD14,PWRD21,PWRD32,PWRMXD,TPMAXD
01025 321* 240  FORMAT(10I,40X,'SAE DRIVING CYCLE D1//'
01025 322* 1 10I,15X,'VMAX=1,F6,3,IMPH(AT TIME1,F6,1,1SEC)!',
01025 323* * 5X,'VELEND=1,F6,3,IMPH1,5X,'DIST',
01025 324* 2 'TRAVELED=1,F6,3,IMILES1,1,24X,'COAST DECEL=1,F6,3,IMPHPS',
01025 325* 3 5X,'BRAKE DECEL=1,F6,3,IMPHPS1'
01025 326* 4 10I,15X,'POWER FROM BATTERY TO OVERCOME AERO RESISTANCE AT TIME1,
01025 327* 5 1,1,7,14,21,28,32 SEC1/1,25X,6F8,3,1KWH1
01025 328* 6 10I,15X,'TOTAL POWER FROM BATTERY AT TIME 1,7,14,21,28,32 SEC1,
01025 329* 7 1 AND MAX1,1,25X,6F8,3,1 KW 1,F8,3,1 (AT TIME1,F6,1,1SEC)1//'
01026 330*  WRITE(6,700)  * HEADING FOR AERO ENERGY REQUIREMENTS
01030 331* 700  FORMAT('1I,T40,1AVG AERO DRAG BATTERY ENERGY REQUIREMENTS (KWH1,
01030 332* 1,1/I)1//10I,T9,1WIND1,T50,1ANGLE OF WIND RELATIVE TO ROAD (DEG)1/
01030 333* 3 1,1,T9,1SPEED1,
01030 334* 4 1,1,T9,1(MPH)1,T16,10I,T22,110I,T28,120I,T34,130I,T40,140I.

```

## PROGRAM LISTING

```

01030 335*      5 T46,'50!,T52,'60!,T58,'70!,T64,'80!,T70,'90!,T75,'100!,  

01030 336*      6 T81,'110!,T87,'120!,T93,'130!,T99,'140!,T105,'150!,T111,'160!,  

01030 337*      7 T117,'170!,T123,'180!,T129,'AVGA//)  

01031 338*      DO 707 M=1,14  

01034 339*      WRITE(6,720) WIND(M),(AEROU(M,L),L=1,19),AEROUA(M)  

01044 340*      720 FORMAT(1 1,'SAE B',F6.2,20F6.4)  

01045 341*      WRITE(6,740) WIND(M),(AEROH(M,L),L=1,19),AEROHA(M)  

01055 342*      740 FORMAT(1 1,'SAE D',F6.2,20F6.4//)  

01056 343*      CONTINUE  

01060 344*      WRITE(6,770)  

01062 345*      770 FORMAT(1 0,'THE FINAL ZERO-WIND CALCULATIONS (FOLLOWING THE 60'  

01062 346*      2 MPH WIND CASE) ARE FOR CD/CDD VALUES VARYING FROM 0.60 TO 1.50 !  

01062 347*      3 / .50X / BY INCREMENTS OF 0.05 AT ZERO WIND. DISREGARD THE YAW !  

01062 348*      4 !HEADING//)  

01063 349*      WRITE(6,800)                                     * HEADING FOR TOTAL ENERGY REQUIREMENTS  

01065 350*      800 FORMAT(1 1,T40,1TOTAL ENERGY REQUIREMENTS (KWH/MI) //  

01065 351*      1 1,T9,1WIND,1T50,1ANGLE OF WIND RELATIVE TO ROAD (DEG) //  

01065 352*      3 1 1,T9,1SPEED!  

01065 353*      4 1 1,T9,1(MPH)!,T16,10!,T22,110!,T28,120!,T34,130!,T40,140!,  

01065 354*      5 T46,'50!,T52,'60!,T58,'70!,T64,'80!,T70,'90!,T75,'100!,  

01065 355*      6 T81,'110!,T87,'120!,T93,'130!,T99,'140!,T105,'150!,T111,'160!,  

01065 356*      7 T117,'170!,T123,'180!,T129,'AVGA//)  

01066 357*      DO 807 M=1,14  

01071 358*      WRITE(6,820) WIND(M),(TOTLU(M,L),L=1,19),TOTLUA(M)  

01101 359*      820 FORMAT(1 1,'SAE B',F6.2,20F6.3)  

01102 360*      WRITE(6,840) WIND(M),(TOTLH(M,L),L=1,19),TOTLHA(M)  

01112 361*      840 FORMAT(1 1,'SAE D',F6.2,20F6.3//)  

01113 362*      CONTINUE  

01115 363*      WRITE(6,870)  

01117 364*      870 FORMAT(1 0,'THE FINAL ZERO-WIND CALCULATIONS (FOLLOWING THE 60'  

01117 365*      2 MPH WIND CASE) ARE FOR CD/CDD VALUES VARYING FROM 0.60 TO 1.50 !  

01117 366*      3 / .50X / BY INCREMENTS OF 0.05 AT ZERO WIND. DISREGARD THE YAW !  

01117 367*      4 !HEADING//)  

01120 368*      WRITE(6,960)  

01122 369*      960 FORMAT(1 1,T40,1ENERGY REQUIREMENTS FOR VARIOUS WIND SPECTRA)  

01122 370*      1 1 1,T55,1(KWH/MILE) //)  

01123 371*      DO 888 IFREQ=1,3                                     * CALC CALC ENERGY REGITS FOR WIND SPECTR  

01126 372*      IF(IFREQ,EQ,1) WINDAV=6.0  

01130 373*      IF(IFREQ,EQ,2) WINDAV=10.0  

01132 374*      IF(IFREQ,EQ,3) WINDAV=18.0  

01134 375*      AAERO=0.0  

01135 376*      AAERO=0.0  

01136 377*      AUTOTL=0.0  

01137 378*      AHOTL=0.0  

01140 379*      DO 9000 II=1,13                                     * WEIGHT ENERGY REGIT PER WIND SPECTRUM  

01143 380*      IF(IFREQ,EQ,1) UFREQ(II)=UFREQ1(II)          * 6 MPH AVG YEARLY WIND SPEED  

01145 381*      IF(IFREQ,EQ,2) UFREQ(II)=UFREQ2(II)          * 10 MPH AVG YEARLY WIND SPEED  

01147 382*      IF(IFREQ,EQ,3) UFREQ(II)=UFREQ3(II)          * 18 MPH AVG YEARLY WIND SPEED  

01151 383*      AAERO=AAERO+AEROUA(II)*UFREQ(II)  

01152 384*      AAERO=AAERO+AEROHA(II)*UFREQ(II)  

01153 385*      AUTOTL=AUTOTL+UFREQ(II)*TOTLUA(II)  

01154 386*      AHOTL=AHOTL+UFREQ(II)*TOTLHA(II)  

01155 387*      900 CONTINUE  

01157 388*      WRITE(6,650) WINDAV,(WIND(M),M=1,13),(UFREQ(N),N=1,13)  

01172 389*      650 FORMAT(1 1,1/T40,1STATISTICAL WIND VELOCITY SPECTRUM WITH 1,  

01172 390*      1 F5.2,1MPH AVERAGE VELOCITY//,T16,1MPH!,13F8.2//,T12,1PORTION!,  

01172 391*      2 13F8.4/

```

## PROGRAM LISTING

## BASE CONDITIONS (Case 3)

### EFFECT OF WIND ON THE PERFORMANCE OF ELECTRIC HYBRID VEHICLES

CASE1 0 4 .3/.45 0 50 0	K2+K3	.0000	.0000
A+H+BETA=AIR DENSITY,L/D	18.000	2500.000	1.035 .002380 1.000
TIRE TYPE: LOW RR RADIAL TIR	C0+C1	.8000=02	.5750=04
	C2+C3	=.2000=05	.2000=07

IM19C1:2,3,4,5,6t 0 4 3015 0 50 0

### PERTINENT ZERO-WIND DRIVING CYCLE QUANTITIES

#### SAE DRIVING CYCLE B

VMAX=19.800MPH(AT TIME 38.08SEC) VELEND= .000MPH DIST TRAVELED= .201MILES  
COAST DFCFL= -.247MPHPS BRAKE DECEL=-3.763MPHPS

POWER FROM BATTERY TO OVERCOME AERO RESISTANCE AT TIME 1.4+9.14+19.21 SEC  
.000 .016 .113 .273 .450 .450kW

TOTAL POWER FROM BATTERY AT TIME 1.4+9.14+19.21 SEC AND MAX  
1.862 5.651 6.296 6.563 5.794 1.625 kW 6.900(AT TIME 7.0SEC)

#### SAE DRIVING CYCLE D

VMAX=45.200MPH(AT TIME 78.0SEC) VELEND= .000MPH DIST TRAVELED= .996MILES  
COAST DFCFL= -.501MPHPS BRAKE DECFL=-4.103MPHPS

POWER FROM BATTERY TO OVERCOME AERO RESISTANCE AT TIME 1.7+14.21+28.32 SEC  
.001 .172 1.180 3.006 4.465 4.465kW

TOTAL POWER FROM BATTERY AT TIME 1.7+14.21+28.32 SEC AND MAX  
3.067 12.619 20.922 20.342 11.917 6.630 kW 21.427 (AT TIME 17.0SEC)

## BASE CONDITIONS (Case 3)

### AVG AERO DRAG BATTERY ENERGY REQUIREMENTS (KWH/MI)

WIND (MPH)	ANGLE OF WIND RELATIVE TO ROAD (DEG)																		AVGA	
	0	10	20	30	40	50	60	70	80	90	100	110	120	130	140	150	160	170	180	
SAE B .00	.0147	.0147	.0147	.0147	.0147	.0147	.0147	.0147	.0147	.0147	.0147	.0147	.0147	.0147	.0147	.0147	.0147	.0147	.0147	.0147
SAE D .00	.0660	.0660	.0660	.0660	.0660	.0660	.0660	.0660	.0660	.0660	.0660	.0660	.0660	.0660	.0660	.0660	.0660	.0660	.0660	.0660
SAE B 5.00	.0236	.0236	.0237	.0238	.0237	.0234	.0229	.0221	.0210	.0196	.0181	.0164	.0147	.0130	.0115	.0101	.0090	.0082	.0079	.0078
SAE D 5.00	.0821	.0820	.0817	.0812	.0803	.0792	.0777	.0758	.0735	.0710	.0682	.0653	.0624	.0596	.0571	.0549	.0532	.0521	.0518	.0509
SAE B 10.00	.0346	.0351	.0360	.0371	.0378	.0377	.0366	.0345	.0315	.0279	.0239	.0199	.0162	.0129	.0101	.0077	.0056	.0040	.0033	.0024
SAE D 10.00	.0999	.1000	.1002	.1001	.0996	.0982	.0960	.0927	.0884	.0833	.0774	.0711	.0647	.0583	.0524	.0472	.0431	.0403	.0393	.0368
SAE B 15.00	.0479	.0490	.0515	.0542	.0559	.0557	.0530	.0479	.0409	.0327	.0245	.0180	.0127	.0085	.0055	.0034	.0021	.0013	.0005	.0300
SAE D 15.00	.1196	.1202	.1214	.1226	.1231	.1221	.1193	.1144	.1076	.0993	.0897	.0796	.0694	.0595	.0502	.0420	.0351	.0304	.0286	.0878
SAE B 20.00	.0633	.0654	.0700	.0749	.0776	.0765	.0706	.0601	.0463	.0345	.0243	.0159	.0094	.0046	.0014	.0004	.0011	.0011	.0010	.0367
SAE D 20.00	.1412	.1425	.1454	.1486	.1505	.1500	.1463	.1391	.1288	.1160	.1019	.0873	.0731	.0600	.0482	.0378	.0289	.0223	.0196	.1004
SAE B 25.00	.0810	.0843	.0917	.0991	.1028	.0998	.0885	.0699	.0524	.0372	.0243	.0138	.0057	.0000	.0035	.0051	.0052	.0043	.0035	.0439
SAE D 25.00	.1646	.1669	.1721	.1778	.1816	.1814	.1761	.1654	.1499	.1311	.1107	.0906	.0723	.0566	.0437	.0328	.0235	.0158	.0122	.1131
SAE B 30.00	.1009	.1057	.1164	.1269	.1313	.1251	.1063	.0811	.0593	.0402	.0240	.0109	.0009	.0061	.0105	.0125	.0125	.0098	.0089	.0513
SAE D 30.00	.1900	.1934	.2015	.2103	.2161	.2159	.2080	.1921	.1693	.1422	.1136	.0865	.0640	.0467	.0335	.0245	.0174	.0105	.0064	.1246
SAE B 35.00	.1230	.1297	.1443	.1581	.1630	.1523	.1239	.0936	.0668	.0432	.0232	.0070	.0054	.0144	.0203	.0232	.0215	.0182	.0171	.0586
SAE D 35.00	.2172	.2222	.2336	.2459	.2539	.2532	.2414	.2183	.1858	.1477	.1106	.0809	.0568	.0382	.0245	.0151	.0092	.0057	.0021	.1363
SAE B 40.00	.1474	.1563	.1753	.1929	.1979	.1813	.1429	.1072	.0747	.0461	.0218	.0019	.0136	.0252	.0332	.0374	.0332	.0295	.0282	.0659
SAE D 40.00	.2464	.2531	.2684	.2848	.2950	.2931	.2759	.2433	.1984	.1496	.1099	.0768	.0505	.0307	.0167	.0078	.0029	.0006	.0009	.1489
SAE B 45.00	.1740	.1854	.2095	.2312	.2360	.2121	.1645	.1218	.0831	.0488	.0196	.0045	.0238	.0386	.0493	.0546	.0478	.0436	.0422	.0731
SAE D 45.00	.2775	.2862	.3060	.3269	.3392	.3354	.3111	.2666	.2063	.1542	.1097	.0731	.0444	.0234	.0093	.0012	.0023	.0029	.0027	.1625
SAE B 50.00	.2030	.2171	.2469	.2731	.2773	.2446	.1877	.1375	.0919	.0514	.0166	.0124	.0360	.0546	.0686	.0728	.0652	.0605	.0590	.0803
SAE D 50.00	.3106	.3216	.3464	.3722	.3867	.3799	.3468	.2877	.2176	.1593	.1097	.0693	.0382	.0158	.0015	.0059	.0080	.0068	.0049	.1769
SAE B 55.00	.2343	.2515	.2876	.3187	.3218	.2788	.2127	.1543	.1010	.0537	.0127	.0218	.0502	.0733	.0911	.0937	.0854	.0803	.0785	.0875
SAE D 55.00	.3457	.3592	.3896	.4207	.4372	.4266	.3826	.3064	.2297	.1647	.1097	.0653	.0314	.0075	.0074	.0144	.0155	.0129	.0096	.1916
SAE B 60.00	.2680	.2886	.3316	.3679	.3696	.3147	.2393	.1720	.1105	.0557	.0080	.0326	.0666	.0947	.1169	.1175	.1083	.1027	.1009	.0946
SAE D 60.00	.3828	.3992	.4357	.4725	.4909	.4754	.4184	.3250	.2425	.1704	.1097	.0609	.0239	.0020	.0179	.0249	.0256	.0202	.0165	.2065
SAE B .00	.0088	.0095	.0103	.0110	.0117	.0125	.0132	.0139	.0147	.0154	.0161	.0169	.0176	.0183	.0191	.0198	.0206	.0213	.0220	.0000
SAE D .00	.0395	.0428	.0461	.0494	.0528	.0561	.0594	.0627	.0660	.0693	.0726	.0760	.0793	.0826	.0859	.0893	.0926	.0959	.0993	.0000

THE FINAL ZERO-WIND CALCULATIONS (FOLLOWING THE 60MPH WIND CASE) ARE FOR CD/CDD VALUES VARYING FROM 0.60 TO 1.50 BY INCREMENTS OF 0.05 AT ZERO WIND. DISREGARD THE YAW HEADING

### BASE CONDITIONS (Case 3)

#### TOTAL ENERGY REQUIREMENTS (KWH/MI)

WIND (MPH)	ANGLE OF WIND RELATIVE TO ROAD (DEG)																			AVGA
	0	10	20	30	40	50	60	70	80	90	100	110	120	130	140	150	160	170	180	
SAE H .00	.169	.169	.169	.169	.169	.169	.169	.169	.169	.169	.169	.169	.169	.169	.169	.169	.169	.169	.169	.169
SAE D .00	.168	.168	.168	.168	.168	.168	.168	.168	.168	.168	.168	.168	.168	.168	.168	.168	.168	.168	.168	.168
SAE H 5.00	.176	.176	.176	.176	.176	.176	.176	.175	.174	.173	.172	.170	.169	.168	.166	.165	.164	.164	.164	.172
SAE D 5.00	.181	.181	.181	.180	.180	.179	.178	.176	.174	.172	.170	.168	.165	.163	.161	.159	.158	.157	.156	.170
SAE H 10.00	.185	.185	.186	.187	.188	.188	.187	.185	.183	.180	.176	.173	.170	.168	.165	.163	.162	.161	.160	.177
SAE D 10.00	.196	.196	.196	.196	.196	.194	.193	.190	.186	.182	.177	.172	.167	.162	.157	.153	.149	.147	.146	.177
SAE H 15.00	.196	.197	.199	.201	.202	.202	.200	.196	.190	.183	.177	.171	.167	.164	.162	.160	.159	.158	.158	.181
SAE D 15.00	.212	.212	.213	.214	.215	.214	.212	.208	.202	.195	.187	.179	.171	.163	.155	.148	.143	.139	.138	.186
SAE H 20.00	.208	.210	.214	.218	.220	.219	.214	.205	.194	.185	.177	.170	.165	.161	.158	.157	.156	.156	.156	.187
SAE D 20.00	.230	.231	.233	.236	.237	.237	.234	.228	.219	.209	.197	.185	.174	.163	.153	.148	.138	.132	.130	.196
SAE H 25.00	.223	.225	.231	.237	.240	.238	.228	.213	.199	.187	.176	.168	.161	.157	.154	.153	.153	.153	.154	.192
SAE D 25.00	.249	.251	.255	.260	.263	.263	.258	.249	.236	.221	.204	.188	.173	.160	.149	.141	.133	.127	.124	.206
SAE H 30.00	.239	.243	.252	.260	.263	.258	.243	.222	.205	.189	.176	.166	.157	.151	.148	.146	.146	.149	.149	.198
SAE D 30.00	.269	.272	.279	.286	.291	.291	.284	.271	.252	.229	.206	.184	.166	.152	.141	.134	.128	.123	.119	.216
SAE H 35.00	.257	.262	.274	.285	.289	.280	.257	.232	.211	.192	.175	.162	.152	.144	.139	.137	.139	.141	.142	.204
SAE D 35.00	.292	.296	.305	.315	.322	.321	.311	.292	.265	.234	.204	.180	.160	.145	.134	.126	.121	.119	.116	.225
SAE H 40.00	.276	.284	.299	.314	.317	.303	.272	.243	.217	.194	.174	.158	.145	.135	.128	.125	.128	.131	.133	.210
SAE D 40.00	.315	.321	.334	.347	.355	.353	.339	.312	.275	.235	.203	.176	.155	.138	.127	.120	.116	.114	.113	.235
SAE H 45.00	.298	.307	.327	.345	.348	.328	.290	.255	.224	.196	.172	.152	.136	.124	.114	.110	.116	.119	.121	.215
SAE D 45.00	.341	.348	.364	.381	.391	.388	.367	.330	.281	.239	.203	.173	.150	.132	.121	.114	.112	.111	.111	.246
SAE H 50.00	.322	.333	.357	.379	.381	.354	.308	.268	.231	.198	.170	.146	.126	.110	.098	.095	.101	.105	.106	.221
SAE D 50.00	.368	.377	.397	.418	.430	.423	.396	.347	.291	.243	.203	.170	.144	.126	.114	.108	.106	.108	.109	.258
SAE H 55.00	.347	.361	.390	.415	.417	.382	.329	.281	.238	.200	.166	.137	.114	.094	.084	.084	.088	.090	.091	.227
SAE D 55.00	.396	.407	.432	.458	.471	.461	.424	.362	.301	.248	.203	.166	.138	.119	.106	.100	.102	.105	.105	.269
SAE H 60.00	.374	.391	.426	.455	.456	.410	.350	.296	.246	.201	.162	.128	.100	.082	.070	.071	.075	.078	.079	.235
SAE D 60.00	.426	.440	.470	.499	.514	.500	.453	.378	.311	.252	.203	.163	.132	.110	.097	.091	.091	.095	.098	.281
SAE H .00	.164	.165	.166	.166	.167	.167	.168	.168	.169	.170	.170	.171	.171	.172	.172	.173	.174	.174	.175	.000
SAE D .00	.147	.149	.152	.155	.157	.160	.163	.165	.168	.171	.173	.176	.179	.181	.184	.187	.189	.192	.195	.000

THE FINAL ZERO-WIND CALCULATIONS (FOLLOWING THE 60MPH WIND CASE) ARE FOR CD/CDO VALUES VARYING FROM 0.60 TO 1.50  
BY INCREMENTS OF 0.05 AT ZERO WIND. DISREGARD THE YAW HEADING

## BASE CONDITIONS (Case 3)

### ENERGY REQUIREMENTS FOR VARIOUS WIND SPECTRA (KWH/MILE)

#### STATISTICAL WIND VELOCITY SPECTRUM WITH 6.00MPH AVERAGE VELOCITY

MPH	.00	5.00	10.00	15.00	20.00	25.00	30.00	35.00	40.00	45.00	50.00	55.00	60.00
PORTION	.1600	.5400	.2500	.0450	.0050	.0000	.0000	.0000	.0000	.0000	.0000	.0000	.0000

FOR ZERO WIND VELOCITY, VELOCITY RANGE IS 0 TO 2.5 MPH  
FOR ALL OTHER VELOCITIES, VELOCITY RANGE IS PLUS AND MINUS 2.5 MPH FROM INDICATED VALUE. SUM OF PORTIONS SHOULD BE 1.0000

#### ENERGY(KWH/MI) REQUIRED TO OVERCOME AERO DRAG AVERAGED OVER EACH DRIVING CYCLE

SAE B1 .0195  
SAE D1 .0715

#### TOTAL ENERGY (KWH/MI) TO TRAVEL EACH SAE CYCLE

SAE B1 .1729  
SAE D1 .1725

#### STATISTICAL WIND VELOCITY SPECTRUM WITH 10.00MPH AVERAGE VELOCITY

MPH	.00	5.00	10.00	15.00	20.00	25.00	30.00	35.00	40.00	45.00	50.00	55.00	60.00
PORTION	.1800	.2500	.2700	.1800	.0600	.0300	.0180	.0080	.0040	.0000	.0000	.0000	.0000

FOR ZERO WIND VELOCITY, VELOCITY RANGE IS 0 TO 2.5 MPH  
FOR ALL OTHER VELOCITIES, VELOCITY RANGE IS PLUS AND MINUS 2.5 MPH FROM INDICATED VALUE. SUM OF PORTIONS SHOULD BE 1.0000

#### ENERGY(KWH/MI) REQUIRED TO OVERCOME AERO DRAG AVERAGED OVER EACH DRIVING CYCLE

SAE B1 .0242  
SAE D1 .0790

#### TOTAL ENERGY (KWH/MI) TO TRAVEL EACH SAE CYCLE

SAE B1 .1766  
SAE D1 .1787

#### STATISTICAL WIND VELOCITY SPECTRUM WITH 18.00MPH AVERAGE VELOCITY

MPH	.00	5.00	10.00	15.00	20.00	25.00	30.00	35.00	40.00	45.00	50.00	55.00	60.00
PORTION	.1500	.1400	.1300	.1200	.1100	.1000	.0800	.0600	.0400	.0300	.0200	.0100	.0100

FOR ZERO WIND VELOCITY, VELOCITY RANGE IS 0 TO 2.5 MPH  
FOR ALL OTHER VELOCITIES, VELOCITY RANGE IS PLUS AND MINUS 2.5 MPH FROM INDICATED VALUE. SUM OF PORTIONS SHOULD BE 1.0000

#### ENERGY(KWH/MI) REQUIRED TO OVERCOME AERO DRAG AVERAGED OVER EACH DRIVING CYCLE

SAE B1 .0357  
SAE D1 .0989

#### TOTAL ENERGY (KWH/MI) TO TRAVEL EACH SAE CYCLE

SAE B1 .1858  
SAE D1 .1948

APPENDIX C  
WIND-WEIGHTING FACTOR EQUATIONS

The EHVSCD computer program described in Section VI and presented in Appendix B was used to determine drag coefficient wind-weighting factors for a large range of vehicle characteristics, wind and driving conditions. Analysis of these results yielded many fortuitous relationships which led to closed-form solutions which can be incorporated into vehicle performance simulators with little effort. The wind-weighting factor,  $F$ , was found to be a linear function of the dominant parameter  $C_{D_{max}}/C_{D_0}$ ; the yaw angle where  $C_{D_{max}}$  occurs is of second order significance.  $F$  is then, in addition, only a function of the annual mean wind speed and the particular driving cycle or constant vehicle speed. The specific equations are given in Tables C-1 and C-2 in Metric and English units, respectively.

Recall that  $F$  is the factor by which the zero-yaw drag coefficient,  $C_{D_0}$ , must be multiplied to yield the effective drag coefficient  $C_{D_{eff}}$ . That is,  $C_{D_{eff}} = F * C_{D_0}$ .

$W$  is the annual mean wind speed which can be chosen by the user with a default value of 12 kph (the average annual mean wind speed in the U.S.). It should be noted that this is not a constant average speed, but rather a statistical average. For instance, an annual mean wind speed of 12 kph has winds of up to 50 kph occurring 3% of the time and winds less than 12 kph occurring 70% of the time (see Figure 12).

$C_{D_{max}}/C_{D_0}$  is the ratio of the maximum yaw-related drag coefficient (which usually occurs at about 30 degrees) to the drag coefficient at zero yaw. The user should be able to input this value. The default values are 1.4 and 1.6 for front windows closed and open, respectively.

Table C-1. Wind-Weighting Factor Equations - Metric Units

---

W = annual mean wind speed in kph

V = vehicle speed in kph

EPA CYCLES

URBAN:

$$F = (1.5 \times 10^{-4}W^2 + 1.5 \times 10^{-2}W)(C_{D_{max}}/C_{D_0}) - 9.3 \times 10^{-3}W + 1.0$$

HIGHWAY:

$$F = (3.6 \times 10^{-4}W^2 + 6.2 \times 10^{-3}W)(C_{D_{max}}/C_{D_0}) - 9.3 \times 10^{-3}W + 1.0$$

SAE ELECTRIC CYCLES (J227a)

B:  $F = (3.5 \times 10^{-4}W^2 + 3.6 \times 10^{-2}W)(C_{D_{max}}/C_{D_0}) - 2.2 \times 10^{-2}W + 1.0$

C:  $F = (4.6 \times 10^{-4}W^2 + 8.9 \times 10^{-3}W)(C_{D_{max}}/C_{D_0}) - 1.1 \times 10^{-2}W + 1.0$

D:  $F = (4.6 \times 10^{-4}W^2 + 3.1 \times 10^{-3}W)(C_{D_{max}}/C_{D_0}) - 1.0 \times 10^{-2}W + 1.0$

CONSTANT SPEED

$$F = [0.98(W/V)^2 + 0.63(W/V)](C_{D_{max}}/C_{D_0}) - 0.40(W/V) + 1.0$$


---

Table C-2. Wind-Weighting Factor Equations - English Units

W = annual mean wind speed in mph

V = vehicle speed in mph

EPA CYCLES

URBAN:

$$F = (3.9 \times 10^{-4}W^2 + 2.4 \times 10^{-2}W)(C_{D_{max}}/C_{D_0}) - 1.5 \times 10^{-2}W + 1.0$$

HIGHWAY:

$$F = (9.3 \times 10^{-4}W^2 + 10^{-2}W)(C_{D_{max}}/C_{D_0}) - 1.5 \times 10^{-2}W + 1.0$$

SAE ELECTRIC CYCLES (J227a)

$$B: F = (9 \times 10^{-4}W^2 + 5.8 \times 10^{-2}W)(C_{D_{max}}/C_{D_0}) - 3.6 \times 10^{-2}W + 1.0$$

$$C: F = (1.2 \times 10^{-3}W^2 + 2.3 \times 10^{-2}W)(C_{D_{max}}/C_{D_0}) - 1.7 \times 10^{-2}W + 1.0$$

$$D: F = (1.2 \times 10^{-3}W^2 + 7.9 \times 10^{-3}W)(C_{D_{max}}/C_{D_0}) - 1.6 \times 10^{-2}W + 1.0$$

CONSTANT SPEED

$$F = [0.98(W/V)^2 + 0.63(W/V)](C_{D_{max}}/C_{D_0}) - 0.40(W/V) + 1.0$$

In the constant speed equation,  $V$  is, of course, the constant vehicle speed. To include the wind-weighting capability in any vehicle performance simulator, only two additional specifications are required by the user: the annual mean wind speed,  $W$ , and the drag-yaw characteristic ratio,  $C_{D_{max}}/C_{D_0}$ . This information along with the previously specified  $C_{D_0}$  or  $C_{D_{eff}}$  A and the specific mission (which defines what F-equation to use) can then be used to calculate a new effective drag coefficient or drag area from

$$C_{D_{eff}} = F * C_{D_0}$$

or

$$C_D A_{eff} = F * C_{D_0} A$$

The user can then set  $C_D = C_{D_{eff}}$  and proceed with all normal simulator calculations.

## APPENDIX D

## AUTOMOTIVE DRAG PREDICTION PROCEDURES

This appendix includes excerpts from three references (13, 14, and 15) detailing procedures for the estimation of automobile drag coefficients. Portions of a fourth reference (16) are also included which may assist in determining the functional relationship between estimated drag coefficients and yaw angles for wind weighting analyses.

Drag Coefficient Estimation (R.G.S. White - Reference 13)

White divides a vehicle into six zones and three subzones for a total of nine categories. These are listed in Table D-1. A rating number is then assigned to the particular vehicle characteristic in each of the nine categories (see Table D-2). These nine intermediate ratings are summed to yield the "drag rating." The resulting drag coefficient is calculated from

$$C_D = 0.16 + (0.0095) \text{ (Drag Rating)}$$

Table D-1. Basic Vehicle Zones (Reference 13)

Zone	Subzone	Category
Front	(a) Outline plan	1
	(b) Elevation	2
Windshield/Roof Junction	(a) Cowl and fender cross section	3
	(b) Windshield plan	4
Roof	(a) Windshield peak	5
	(b) Roof plan	6
Rear Roof/Trunk		7
Lower Rearend		8
Underbody		9

Table D-2. Drag Rating System\*

<u>Category 1. Front End Plan Outline</u>	<u>Rating</u>
Approximately semicircular	1
Well-rounded outer quarters	2
Rounded corners without protuberances	3
Rounded corners with protuberances <sup>(a)</sup>	4
Squared tapering-in corners	5
Squared constant-width front	6
<u>Category 2. Elevation<sup>(b)</sup></u>	<u>Rating</u>
(a) Low rounded front, sloping up	1
(b) High tapered rounded hood	
(a) Low squared front, sloping up	2
(b) High tapered squared hood	
Medium height rounded front, sloping up	3
(a) Medium height squared front, sloping up	4
(b) High rounded front, with horizontal hood	
High squared front, with horizontal hood	5

\* Adapted from Reference 13.

Table D-2. Drag Rating System (contd)

<u>Category 3. Cowl and fender cross-section - windshield/roof junction</u>	<u>Rating</u>
Flush hood and fenders, well-rounded body sides	1
High cowl, low fenders	2
(a) Hood flush with rounded-top fenders	3
(b) High cowl, with rounded-top fenders	4
Hood flush with squared-edged fenders	4
Depressed hood, with high squared-edged fenders	5
<u>Category 4. Windshield plan<sup>(c)</sup></u>	<u>Rating</u>
Full-wrap-around (approximately semicircular)	1
Wrapped-round ends	2
Bowed	3
Flat	4
<u>Category 5. Windshield peak</u>	<u>Rating</u>
Rounded	1
Squared (including flanges or gutters)	2
Forward-projecting peak	3

Table D-2. Drag Rating System (contd)

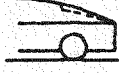
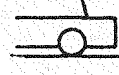
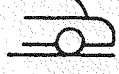
<u>Category 6. Roof plan</u>	<u>Rating</u>
Well- or medium-tapered to rear	 1
Tapering to front and rear (max. width at BC post) or approximately constant width	 2
Tapering to front (max. width at rear)	 3
<u>Category 7. Rear roof/trunk<sup>(d)</sup></u>	<u>Rating</u>
Fastback (roof line continuous to tail)	 1
Semi fastback (with discontinuity in line to tail)	 2
Squared roof with trunk rear edge squared	 3
(a) Rounded roof with rounded trunk	 4
(b) Squared roof with short or no trunk	 4
Rounded roof with short or no trunk	 5

Table D-2. Drag Rating System (contd)

<u>Category 8. Lower Rear End</u>	<u>Rating</u>
Well- or medium-tapered to rear	1
Small taper to rear or constant width	2
Outward taper (or flared-out fins)	3
<u>Category 9. Underbody (e)</u>	<u>Rating</u>
Integral, flush floor, little projecting mechanism	1
Intermediate	2
Integral, projecting structure and mechanism	3
Intermediate	4
Deep chassis	5

- (a) Fender mirrors. Include in protuberances if at the fender leading end. Otherwise add 1.
- (b) Add: 3 for separate fenders; 4 for open front to fenders (above bumper level); 2 for raised built-in headlamps; 4 for small separate headlamps; 7 for large separate headlamps.
- (c) Add: 1 for upright windshield; 1 for prominent flanges or rain gutters.
- (d) Add: 3 for high fins or sharp longitudinal edges to trunk; 2 for separate fenders. Note: In all the ratings in this column, the trunk is assumed to be rounded laterally.
- (e) Intermediate ratings applied from vehicle examination.

NOTE: Throughout table, the word "taper" or "tapered" refers to the plan view.

Drag Coefficient Estimation (J. J. Cornish)

Cornish divides a vehicle into 10 zones and assigns a sub-rating of from 1 to 3 to each of them (see Table D-3). The total rating, R, is the sum of these 10 sub-ratings. Two windshield zone items (numbers 4 and 5) refer to the elevation and plan views, respectively. The resulting drag coefficient is calculated from

$$C_D = 0.62 - (0.01) (R)$$

Table D-3. Aerodynamic Rating

No.	Item	1	2	3
1	Grill	Blunt; square	Fairly sloped	Well sloped
2	Lights	Open; exposed	Partially inset	Well faired
3	Hood	Flat	Fairly sloped	Convex, sloped
4	Windshield	Steep	Fairly sloped	well sloped
5	Windshield	Flat	Fairly curved	Well curved
6	Roof top	Open	Fairly sloped	Convex, sloped
7	Rear Window	Notched	Fairly sloped	Fastback type
8	Trunk	Cut off square	Fairly sloped	Fastback type
9	Wheels	Exposed	Partially closed	Well concealed
10	Underside	Exposed	Partial pan	Full pan

### Drag Coefficient Estimation (B. Pershing)

This procedure is much more complicated but much less subjective than the previous two. The relevant vehicle dimensions and areas are illustrated in Figures D-1 and D-2. The total drag coefficient is defined as the summation of eleven component coefficients:

$$C_D = \sum_{i=1}^{11} C_{D_i}$$

The details of the determination of the  $i$ th components follow (reproduced directly from Reference 15):

#### Front End Drag Coefficient, $C_{D_1}$

$$C_{D_1} = 0.707 \left( \frac{A_F}{A_R} \right) \left\{ 1.0 - 2.79 \left( \frac{R}{E} \right)_u + 0.82 \left( \frac{R}{E} \right)_1 - 5.21 \left( \frac{R}{E} \right)_v \right. \\ \left. - 29.5 \left( \frac{R}{E} \right)_u \left( \frac{R}{E} \right)_1 \left[ 1.0 - 2.25 \left( \frac{R}{E} \right)_v \right] \right\}$$

where

$A_F$  = front end projected area,  $\text{m}^2$  ( $\text{ft}^2$ )

$R$  = edge radius,  $\text{m}$  ( $\text{ft}$ )

$E$  = running length of the edge radius,  $\text{m}$  ( $\text{ft}$ )

and the subscripts  $u$ ,  $1$ , and  $v$  refer to the upper, lower, and vertical edges of the front end, respectively. The  $(R/E)_i$  are to be taken as 0.105 when the estimated values exceed this magnitude.

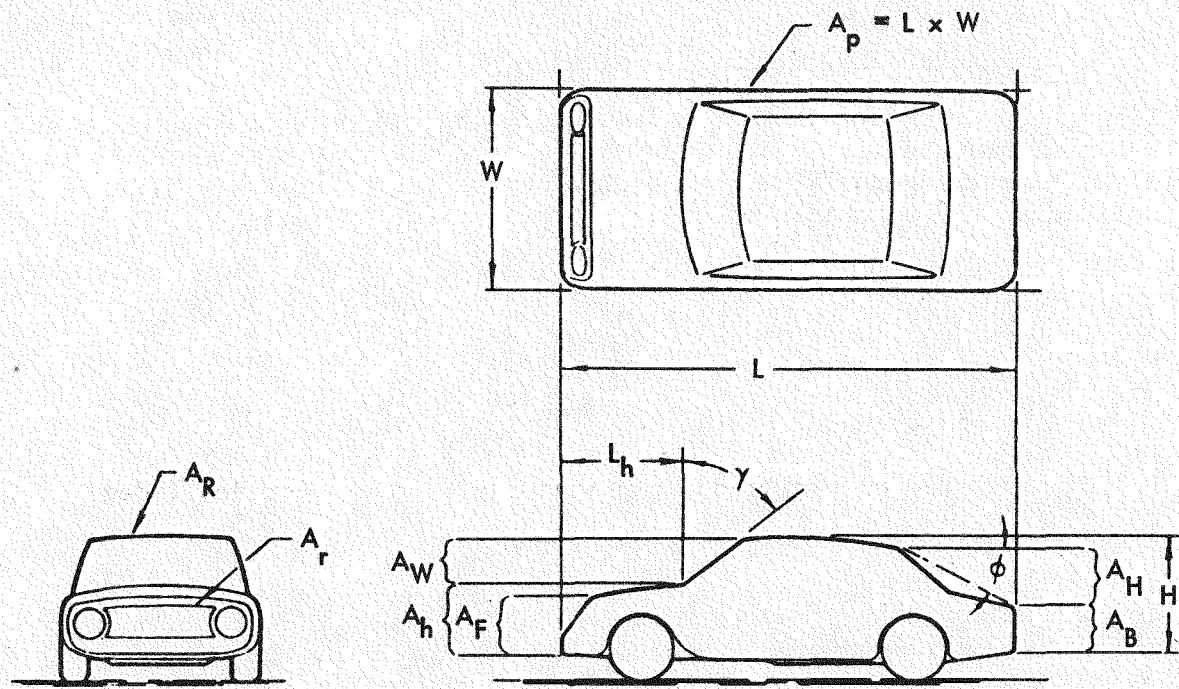


Figure D-1. Vehicle Dimensions (Reference 15)

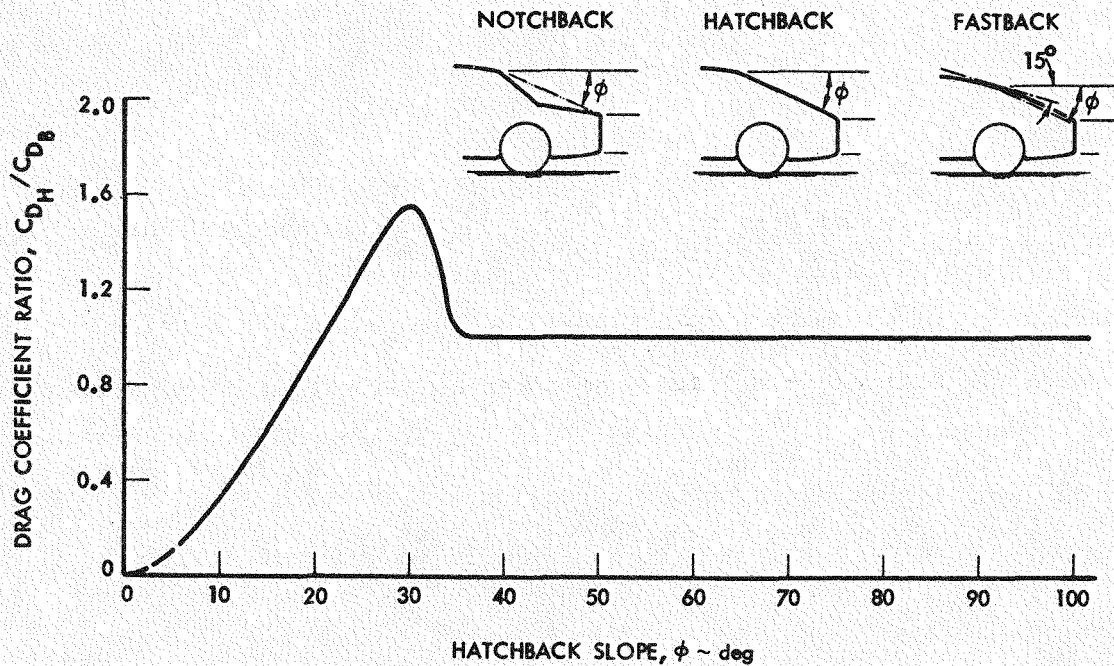


Figure D-2. Hatchback-Notchback Drag Coefficient Ratio

Windshield Drag Coefficient,  $C_{D_2}$  -

$$C_{D_2} = 0.707 \left( \frac{A_W}{A_R} \right) \left[ 1.0 - 2.79 \left( \frac{R}{E} \right)_u, \cos \beta - 5.21 \left( \frac{R}{E} \right)_v, \right] \cos^2 \gamma$$

where

$A_W$  = projected area of windshield,  $m^2$  ( $ft^2$ )

$\gamma$  = slope of the windshield measured from the vertical, deg

$\beta = 2\gamma$

and the subscripts  $u'$  and  $v'$  refer to the roof-windshield intersection and the windshield posts, respectively. The value of  $\cos \beta$  is to be taken as zero for  $\gamma$  larger than 45 degrees and the  $(R/E)_i$  are to be taken as 0.105 for estimated values exceeding this magnitude.

Front Hood Drag Coefficient,  $C_{D_3}$  -

$$C_{D_3} = 0.707 \left( \frac{A_h - A_F}{L_h} \right)^2 / A_R$$

where

$A_h$  = projected area of body below the hood-windshield intersection,  $m^2$  ( $ft^2$ )

$L_h$  = length of hood in the elevation or side view,  $m$  ( $ft$ )

and the quantity  $(A_h - A_F)$  is to be taken as zero if it is negative.

Rear Vertical Edge Drag Coefficient,  $C_{D_4}$

$$C_{D_4} = -0.19 \left( \frac{R_v}{W} \right) \left( \frac{E_b}{H} \right) \text{ for } \left( \frac{R_v}{W} \right) \leq 0.105$$

$$= -0.02 \left( \frac{E_b}{H} \right) \text{ for } \left( \frac{R_v}{W} \right) > 0.105$$

where

$R_v$  = radius of rear vertical edges, m (ft)

$W$  = vehicle width, m (ft)

$E_b$  = length of rear vertical edge radius, m (ft)

$H$  = vehicle height, m (ft)

Base Region Drag Coefficient,  $C_{D_5}$

$$C_{D_5} = 0.15 \left[ \left( \frac{A_B}{A_R} \right) + \left( \frac{C_{D_H}}{C_{D_B}} \right) \left( \frac{A_H}{A_R} \right) \right]$$

where

$A_B$  = projected area of flat portion of base region

$A_H$  = projected area of upper rear or hatch portion of base region measured from the upper rear roof break (or for smoothly curved rooflines, that point where the roofline slope is 15 degrees) to the top of the flat base,  $\text{m}^2$  ( $\text{ft}^2$ )

$C_{D_B}$  = drag coefficient of the flat base

$C_{D_H}$  = drag coefficient of the upper rear or hatch portion of the base region

and the ratio  $(C_{D_H} / C_{D_B})$  is shown in Figure D-2 as a function of  $\phi$ , the angle of the line from the upper rear roof break to the top of the flat base as measured from the horizontal.

Underbody Drag Coefficient,  $C_{D_6}$

$$C_{D_6} = 0.025 (0.5 - x/L) \left( \frac{A_p}{A_R} \right) \text{ for } 0 \leq x/L \leq 0.5$$
$$= 0 \quad \text{for } x/L > 0.5$$

where

$x$  = smoothed forward length of the underbody, m (ft)

$L$  = vehicle length, m (ft)

$A_p$  = projected plan area of the vehicle,  $m^2$  ( $ft^2$ )<sup>2</sup>

Wheel and Wheel Well Drag Coefficient,  $C_{D_7}$

$$C_{D_7} = 0.14$$

Rear Wheel Well Fairing Drag Coefficient,  $C_{D_8}$

$$C_{D_8} = -0.01$$

Protuberance Drag Coefficient,  $C_{D_9}$

$$C_{D_9} = \frac{1.1}{A_R} \sum A_{p_j}$$

where

$A_{p_j}$  = projected area of  $j^{\text{th}}$  protuberance,  $\text{m}^2$  ( $\text{ft}^2$ )

Bullet Mirror Drag Coefficient,  $C_{D_{10}}$

$$C_{D_{10}} = 0.4 \frac{A_M}{A_R}$$

where

$A_M$  = projected area of mirror with bullet fairing,  $\text{m}^2$  ( $\text{ft}^2$ )

Cooling Drag Coefficient,  $C_{D_{11}}$

$$C_{D_{11}} = 1.8 \left( \frac{A_r}{A_R} \right) \left( \frac{u_r}{u} \right) \left[ 1.0 - 0.75 \left( \frac{u_r}{u} \right) \right]$$

where

$A_r$  = radiator area,  $\text{m}^2$  ( $\text{ft}^2$ )

$u_r$  = exit velocity of cooling air from radiator

$$(u_r/u) = 0.233 \left[ 1.0 - k (u/100)^2 \right]$$

and

$$k = 1.146 (\text{m/sec})^{-2} \quad \left[ \text{or } 0.299 (\text{mph})^{-2} \right]$$

Drag Coefficient versus Yaw Angle (W. D. Bowman - Reference 16)

Bowman has developed this generalized equation describing the functional relationship between drag coefficient and yaw angle:

$$C_D = C_{D_0} + K_1 (1 - \cos 6\psi)$$

where  $C_{D_0}$  is the drag coefficient at zero yaw angle,  $\psi$  is the yaw angle and  $K_1$  is a factor dependent upon  $C_{D_0}$ . Table D-4 describes the relationship.

Table D-4

Vehicle Description	$C_{D_0}$	$K_1$
Unstreamlined sedans of harsh, angular character with cowled or hooded elements around nose. Sedans with full width or full height grill openings and minimal camber at hood leading edge.	0.56-0.49	0.038-0.053
Unstreamlined notchback sedans with partial height grill openings, cambered hood and fender leading edges.	0.49-0.45	0.53-0.01
Bustleback and fastback sedan forms with filleted body surface intersections. Partial width and/or height grill openings. Well rounded corners and extremities.	0.45-0.40	0.01-0.03
Well streamlined racing coupes and fastback forms, smooth body surfaces. Well rounded or parabolic nose forms.	0.40-0.27	0.03-0.02